

ECOGRAPHY

Living on the edge - physiological tolerance to frost and drought explains range limits of 35 European tree species

Journal:	<i>Ecography</i>
Manuscript ID	ECOG-07528.R1
Wiley - Manuscript type:	Research Article
Keywords:	safety margins, physiological limits, P50, LT50, minimum soil water potential, species distribution
Abstract:	<p>1. Species distribution models are key to evaluate how climate change threatens European forests and tree species distributions. However, current models struggle to integrate ecophysiological processes. Mechanistic models are complex and have high parameter requirements. Some correlative species distribution models have tried to include traits but so far have struggled to directly connect to ecophysiological processes. Here, we propose a new strategy in which species distributions are based on safety margins which represent species' proximity to their physiological thresholds.</p> <p>2. We derived frost and drought safety margins for 38 European tree species as the difference between physiological tolerance traits and local maximum stress. We used LT50 and P50 as tolerance traits for frost and drought, respectively, and local minimum temperature and minimum soil water potential as maximum stress. We integrated these safety margins into a species distribution model, which tests if the probability of species presence declines rapidly when the safety margin reaches zero, when physiological stress exceeds the species' tolerance traits.</p> <p>3. Our results showed that 35 of the 38 studied species had their distribution explained by one or both safety margins. We demonstrated that safety-margins-based model can be efficiently transferred to species for which occurrence data are not available.</p> <p>4. The probability of presence dropped dramatically when the frost safety margin reached zero, whereas it was less sensitive to the drought safety margin. This differential sensitivity may be due to the more complex regulation of drought stress, especially as water is a shared resource, whereas frost is not.</p> <p>5. Our analysis provides a new approach to link species distributions to their physiological limits and shows that, in Europe, frost and drought safety margins are important determinants of species distributions.</p>

- ¹ Living on the edge - physiological tolerance to frost and drought
² explains range limits of 35 European tree species

³

⁴ —

⁵

⁶ 1. ~~Models~~ Species distribution models are key to evaluate how climate change
⁷ threatens European forests and tree species distributions. However, current
⁸ ~~species distribution~~ models struggle to integrate ecophysiological processes. Mech-
⁹ anistic models are complex and have high parameter requirements. Some corre-
¹⁰ lative species distribution models have tried to include traits but so far have failed
¹¹ struggled to directly connect to ecophysiological processes. Here, we propose an
¹² intermediate strategy where a new strategy in which species distributions are
¹³ based on their safety margins which represent their species' proximity to their
¹⁴ physiological thresholds.

¹⁵ 2. We derived frost and drought safety margins for 38 European tree species as the
¹⁶ difference between physiological tolerance traits and local maximum stress. We
¹⁷ used LT_{50} and Ψ_{50} as tolerance traits for frost and drought, respectively, and lo-
¹⁸ cal minimum temperature and minimum soil water potential as maximum stress.
¹⁹ We integrated these safety margins into a species distribution model, which tests
²⁰ if the probability of species presence declines rapidly when the safety margin
²¹ reaches zero, when physiological stress exceeds the species' tolerance traits.

²² 3. Our results showed that 35 of the 38 studied species had their distribution
²³ explained by one or both safety margins. We demonstrated that safety-margins-
²⁴ based model can be efficiently transferred to species for which occurrence data
²⁵ are not available.

²⁶ 4. The probability of presence dropped dramatically when the frost safety mar-
²⁷ gin reached zero, whereas it was less sensitive to the drought safety margin. This
²⁸ differential sensitivity may be due to the more complex regulation of drought
²⁹ stress, especially as water is a shared resource, whereas frost is not. ~~However, we~~
³⁰ ~~did not find a clear effect of local competition hierarchy on the response to safety~~
³¹ ~~margin, but competition needs further analysis.~~

³² 5. Our analysis provides a new approach to link species distributions to their
³³ physiological limits and shows that, in Europe, frost and drought safety margins
³⁴ are important determinants of species distributions.

³⁵ keywords: Physiological limits | Tolerance traits | LT_{50} | P_{50} | Safety margins | Minimum soil water
³⁶ potential | Minimum temperature | Species distribution

³⁷

38 Introduction

39 Climate change is a major threat to European forests and has already led to significant changes in species
40 ranges, forest structure and consequently ecosystem services (Lindner et al., 2014). A common way to as-
41 sess this vulnerability is through correlative Species Distribution Models (SDMs), which correlate species
42 occurrence data with climate drivers to estimate shifts in species distributions (Elith and Leathwick,
43 2009). However, the advent of new climatic conditions, particularly at the hot edge of species distri-
44 butions, leads to extrapolation of SDM outside their calibration range, often resulting in low predictive
45 performance (Nguyen and Leung, 2022). To overcome extrapolation issues, mechanistic models attempt
46 to explicitly represent key physiological processes that control species persistence (Chuine and Beaubien,
47 2001; Ruffault et al., 2022; Venturas et al., 2021). Despite increasing transferability in time and space,
48 mechanistic models require extensive parameter estimation for each species, which limits their application
49 to a few species (Dormann et al., 2012). This is why recent research has sought to integrate plant func-
50 tional traits into correlative SDMs in order to include external information on species ecological strategies
51 and connect SDMs with mechanistic models (Pollock et al., 2012; Vesk et al., 2021). In this approach (re-
52 ferred hereafter as traits-SDM) functional traits modulate ~~the response of species~~ species' response to the
53 environment, which facilitates the transfer of models to species for which only the traits are known (Vesk
54 et al., 2021). Yet the processes determining the trait-environment relationship are usually not explicit
55 and are inferred only in post-hoc analyses. This is mostly because the traits that are commonly measured
56 and classically used in traits-SDM, such as specific leaf area, maximum height, or wood density (Pollock
57 et al., 2012), are integrative traits that have complex drivers and are not directly linked to environmental
58 constraints. Because of this, connecting ~~these traits-SDM~~ models with the mechanistic ecophysiological
59 processes controlling species distribution remains difficult.

60 In recent years, there has been an increased availability in physiological tolerance traits that directly
61 quantify the tolerance thresholds of ~~the~~ plants. These new traits offer a path to a tighter connection with
62 ecophysiological processes, but this requires moving SDMs from classical climate space to the space of
63 the physiological stress experienced by the species (Choat et al., 2018; Dormann et al., 2012). To do this,
64 one way is to convert the environmental drivers into physiological stresses: the distance between the local
65 maximum physiological stress and the physiological tolerance trait of the species defines a safety margin,
66 i.e. a quantification of the local risk of crossing an ecophysiological limit (Martínez-Vilalta et al., 2021).

67 Fitting correlative SDMs in this safety margins space would enable to link directly traits to physiological
68 processes without modelling the full complexity of ecophysiological processes. More specifically, this
69 would allow us to test if species' probability of presence decreases as they approach their physiological
70 limits in safety margin space. In this approach, model parameters would be directly linked to traits, in
71 particular, quantify whether excessive stress (i.e. negative safety margin) induces a drop in probability of
72 presence. Such a safety margin-based model would provide a foundation for a generic species distribution
73 model, which would enable to predict ~~the distribution of species based solely on species's distributions~~ solely
74 based on their traits.

75 In Europe, frost and drought are primary physiological stresses shaping tree species distributions
76 (Lindner et al., 2014). These stresses act through multiple physiological processes (Anderegg et al., 2015;
77 Körner et al., 2016), thus species' tolerance to frost and drought can be tricky to capture.

78 Concerning frost, it can reduce fitness because freeze-thaw cycles lead to hydraulic failure or because
79 low temperatures provoke extracellular ice causing cell lysis and tissue death both in spring and in winter
80 (Körner et al., 2016; Sakai and Larcher, 1987). There are currently no ~~standardized~~ standardised traits for
81 comparing resistance to freeze-thaw-induced embolism across a large number of species (Charrier et al.,
82 2017). Cell tolerance to cold-induced lysis can be measured as the temperature at which 50% of cells are
83 lysed, so-called LT_{50} . It is a dynamic trait that decreases during cold acclimation, reaches a minimum
84 value in deep winter and then rises during cold deacclimation in spring (Charrier et al., 2013, 2017; Sakai
85 and Larcher, 1987). This temporal dynamics makes it more difficult to measure LT_{50} in a standardised
86 way during spring for a large number of species, as it largely depends on local temperature dynamics,
87 whereas standardisation is easier for winter LT_{50} . We propose here to focus on winter maximum frost
88 hardiness, considering this trait as static in contrast with tolerance to spring frost events and freeze-thaw
89 induced embolism.

90 Concerning drought, it can cause stomata ~~to close~~ closure and limit growth (Martin-StPaul et al.,
91 2017), or inflict excessive tension on the plant's water column, causing embolism of the conduits and
92 leading to hydraulic failure. The latter is often recognised as a major cause of forest mortality during
93 severe drought (Anderegg et al., 2015) (but see Mantova et al., 2022 Mantova et al. (2022) for a debate
94 about the exact mechanisms at play). Ψ_{50} is a trait that assesses plants' resistance to hydraulic failure by
95 measuring the water potential that causes a 50% loss in hydraulic conductivity due to drought-induced
96 embolism. We now have large databases on Ψ_{50} allowing the classification of species resistance to drought-

97 induced hydraulic failure (Choat et al., 2012; Hammond et al., 2021; Martin-StPaul et al., 2017).

98 To our knowledge, no studies have explored direct links between LT_{50} and Ψ_{50} and species distribution.
99 Yet, several studies have shown correlations of LT_{50} and Ψ_{50} with stress-induced mortality (Anderegg
100 et al., 2015; Charra-Vaskou et al., 2012; Trugman et al., 2021), although this has been done only for
101 a few species for ~~the~~ LT_{50} (*Scots pine*, Lindström et al., 2014; *Douglas-fir*, Timmis et al., 1994). Some
102 studies have also reported correlations between Ψ_{50} or LT_{50} and species mean climate or rough indicators
103 of species climatic range limits (Charrier et al., 2013; Larter et al., 2017; Sanchez-Martinez et al., 2020;
104 Skelton et al., 2021). Most of these studies were not based on explicit estimation of safety margin but just
105 on classical climatic variables. More recently, some studies have modelled the risk of drought hydraulic
106 damage at the tree level in the US (Venturas et al., 2021, with a mechanistic model) or in France and
107 Spain (Benito Garzón et al., 2018, with drought safety margins) and found it to explain, respectively,
108 2% and 27% of the variance in mortality. Sanchez-Martinez et al. (2023) assessed drought hydraulic risk
109 at the community level (based on phylogenetically imputed species average safety margins) and found
110 a significant relationship with drought-induced mortality. Some studies have explored the relationship
111 between the spring frost safety margin and species' upper elevation limits for a few tree species in the
112 Alps (Lenz et al., 2013). But to our knowledge, no studies have used both frost and drought tolerance
113 traits to build SDMs in a multidimensional safety margin space at the continental scale.

114 ~~Finally, observed distribution data reflects realised niches constrained by abiotic stresses but also
115 biotic interactions, such as competition. This is important in forests where competition for light is fierce,
116 particularly in areas of high productivity. Indeed, competition for light could lead to a drop in the
117 probability of presence before physiological tolerance thresholds are reached.~~

118 Here we propose to build on recent advances in the measurement of Ψ_{50} and LT_{50} , together with
119 the availability of large-scale climate data (Muñoz-Sabater et al., 2021), to derive continent-wide frost
120 and drought safety margins across Europe for 38 European tree species. When included in a SDM, this
121 allows us to test whether there is a sudden drop in the probability of presence when a species crosses
122 its threshold of zero safety margin, *i.e.* when the physiological stress exceeds its tolerance (Fig. 1), and
123 therefore whether Ψ_{50} and LT_{50} are relevant to delineate species distributions. More specifically, our
124 analysis tests the following hypotheses: (i) species' maximum experienced frost or drought stress better
125 explains the interspecific variation in LT_{50} and Ψ_{50} than classical climatic variables; (ii) parameters of
126 the fitted SDM indicate a drastic and non-linear drop in the probability of species presence as the safety

127 margins decrease, and the drop occurs at the zero safety margins of the species; (iii) models based on safety
128 margins can be transferred to species with only traits and no occurrence to predict their distribution;~~(iv)~~
129 ~~species dominant in the local light competitive hierarchy (as indicated by their position the hierarchy of~~
130 ~~species shade tolerance) are more likely to have their distributions directly limited by their safety margins~~
131 ~~and therefore show a more non-linear drop in probability of presence at the zero safety margin.~~

132 Material and methods

133 We compiled published data on drought and frost physiological tolerance traits for the main European
134 tree species and complemented missing species with new measurements. Using climate reanalysis and
135 soil hydraulic parameter maps, we computed proxies of long-term maximum frost or drought stress for
136 all cells of a European tree species occurrence database. These allowed us to estimate both species'
137 maximum experienced drought and frost stress throughout their distribution and how species-specific
138 safety margins vary within the species distribution. These safety margins were used to build bivariate
139 logistic species distribution models (Fig. 1).

140 Study area and species presence data

141 The study was carried out on 38 tree species naturally occurring in Europe (Supporting Information,
142 SI Table S1 and S2) for which physiological traits and more than 400 occurrence points were available.
143 These species are distributed in forest biomes ranging from the Mediterranean to the boreal forest.

144 Physiological Tolerance Thresholds for Frost and Drought

145 Species-specific stress tolerance traits are estimated as the level of stress at which irreversible damage
146 is reached (generally 50% of damage). They are extracted from sigmoid vulnerability curves fitted to
147 experimental data of damage measurements at different stress levels. For each species, we took the
148 average of all measurements from our compilation of published data and additional measurements (see
149 details per traits below).

150 **Frost Tolerance**

151 We collected estimates of LT_{50} (the temperature causing 50% of cell lysis) from various published and
152 unpublished data (see SI1). As we focused on winter frost tolerance to control for seasonal variation in
153 frost tolerance (LT_{50}), we used measurements taken in winter, when all species exhibit maximum frost
154 tolerance. We selected only measurements that were performed using either the electrolyte leakage or
155 visual scoring method, on adult trees, and on branches or buds. For 23 species for which LT_{50} data
156 were not available in the literature or of low quality, additional measurements were made to complete the
157 database (see Table S1 for details).

158 **Drought Tolerance**

159 We extracted from global databases estimates of the xylem pressure (*i.e.* water potential) at which the
160 percentage of embolized conduits exceeds the critical threshold of hydraulic failure (Choat et al., 2012;
161 Hammond et al., 2021; Martin-StPaul et al., 2017, see SI1 and Table S2) (Ψ_{crit}). We filtered out Ψ_{crit}
162 measurements with non-sigmoid vulnerability curves. We chose measurements from adult tree stems to
163 avoid the ontogenetic effects observed with saplings grown in pots. Previous studies have suggested that
164 the threshold of embolism leading to hydraulic failure differs between gymnosperms and angiosperms
165 (Urli et al., 2013). Based on this, we used a critical threshold of 50% for gymnosperms (Ψ_{50}) and 88%
166 for angiosperms (Ψ_{88}) as the point of no return.

167 **Estimation of long-term maximum stresses and safety margins**

168 The Frost and Drought Hydraulic Safety Margin (FSM, HSM) are the difference between the physiological
169 tolerance threshold and the long-term maximum experienced stress at a given location.

170 There are several approaches to estimating frost and drought maximum stress. For frost, the maximum
171 stress is related to the extreme minimum temperature (even during a short period and with a long return
172 interval). Thus, we used long-term hourly temperature reanalysis time series to extract extreme low-
173 temperature events. We acknowledge that the temperature experienced by a tree can deviate from air
174 temperature by several degrees, but no data allows us to go into such detail for the moment. For drought,
175 the minimum tree water potential at midday - measured in the field - is most commonly used as a proxy
176 for maximum stress and compared to Ψ_{crit} (Choat et al., 2012; Sanchez-Martinez et al., 2023). However,

177 this approach cannot be used at the scale of a species' distribution because minimum water potentials
 178 are only available for a few locations. Instead, we determined the maximum drought stress based on the
 179 minimum soil water potential (Ψ_{min}) from long-term reanalysis of soil water content (θ). Assuming that
 180 tree and soil water potentials are in equilibrium when stomata are closed to control water loss, Ψ_{min} is
 181 a proxy for the maximum experienced stress (Martínez-Vilalta et al., 2021).

182 Long-term climatic minimum

183 We used hourly time series of temperature and soil water content (θ) between 1984 and 2021 taken from
 184 the ERA5 Land dataset at 9x9km resolution (Muñoz-Sabater et al., 2021). For each variable, location
 185 and year, we computed the annual maximum stress as the minimum of the annual time series. Then to
 186 estimate the long-term maximum stress of frost and drought (T_{min} and θ_{min}) while limiting the effect
 187 of outliers, we computed the 5th percentile of the time series of annual minimum of temperature and θ .
 188 The 5th percentile is equivalent to a 20-years return rate.

189 Derivation of minimum soil water potential from soil water content

190 Ψ_{min} depends on the minimum soil water content (θ_{min}), soil hydraulic properties (mainly driven by
 191 texture) at each location, and root distribution. For each of the four soil horizons (ranging from 0 to
 192 2.8m) and cell of the ERA5 Land dataset (Muñoz-Sabater et al., 2021) we computed θ_{min} with the
 193 method presented above. Then, we used the Van Genuchten pedotransfer functions to calculate Ψ_{min} for
 194 each horizon h (Van Genuchten, 1980, SI3, Fig. S2) using the following equation:

$$\bar{\theta}_{min,h} = \frac{\theta_{min,h} - \theta_r}{\theta_s - \theta_r} \quad (1)$$

$$\Psi_{min,h} = [(\frac{1}{\bar{\theta}_{min,h}})^{1/m} - 1]^{1/n} * \frac{1}{\alpha} \quad (2)$$

195 Where $\theta_{min,h}$ is the minimum soil water content, $\bar{\theta}_{min,h}$ is the reduced water content, $\theta_r, \theta_s, \alpha, n$ and
 196 m are hydraulic parameters. We extracted hydraulic parameters from Tóth et al. (2017) 1x1km soil
 197 hydraulic parameter maps, which provide parameters for seven horizons from 0 to 2.8 metres deep based
 198 on soil information data. We matched each of the latter seven horizons to one of the four horizons from
 199 ERA5 land (see details in SI, Table S3).

200 We used the root module of the SurEau-ECOS model (Ruffault et al., 2022) to weight the contribution of
 201 the water potential of each horizon based on their hydraulic conductivity and fine roots density distribu-
 202 tion to compute a value close to the soil water potential experienced by the tree root system. First, using
 203 the Van Genuchten hydraulic conductivity curve, we calculated the unsaturated hydraulic conductivity
 204 of each horizon h , where :

$$K_{min,h} = K_0 \cdot (\bar{\theta}_{min,h})^L \cdot (1 - (1 - \bar{\theta}_{min,h}^{1/m}))^m \quad (3)$$

205 With K_0 , m and L hydraulic parameters extracted from (Tóth et al., 2017). Then, K_{min} was scaled to
 206 the width of the layer using the Gardner-Cowan coefficient, B_{GC} (see details in SI4.1). B_{GC} modulates
 207 the conductance of the soil layer according to the density of fine roots in the layer; it depends on the
 208 root radius, the root distribution profile (depending on a root distribution index β , details in SI4.1),
 209 the root-to-leaf ratio, the leaf area index (LAI) and the maximum root depth at each location. Root
 210 radius, root-to-leaf ratio and LAI were set to 0.004m, 1 and $5m^2/m^2$ respectively, according to the
 211 parameterization of SUREAU-ECOS (Ruffault et al., 2022). The maximum root depth at 1x1km was
 212 extracted from Hiederer (2013). Detailed calculation and sensitivity analysis of Ψ_{min} to B_{GC} parameters
 213 (LAI and β) are presented in SI3. For each horizon h the rescaled potential was :

$$\Psi_{root,h} = \Psi_{min,h} \cdot K_{min,h} \cdot B_{CG,h} \quad (4)$$

214 Finally, $\Psi_{root,h}$ was computed for each horizon and then scaled to the total conductivity. The weighted
 215 Ψ_{min} experienced by the roots over the entire soil profile was :

$$\Psi_{min} = \frac{\sum_{h=1}^7 [\Psi_{min,h} \cdot K_{min,h} \cdot B_{CG,h}]}{\sum_{h=1}^7 [K_{min,h}]} \quad (5)$$

216 **Species distribution analysis**

217 **Presence/absence and climate data**

218 We extracted presence/absence data from the EuForest database (Mauri et al., 2017), which is a 1x1km
219 grid, based on aggregated datasets. For each EuForest occurrence point, in addition to T_{min} and Ψ_{min} ,
220 we extracted from the CHELSA data (Karger et al., 2017) the annual sum of precipitation *map*, annual
221 potential evapotranspiration *pet* and mean annual temperature *mat*. In order to ensure that differences
222 in the resolution of the climatic data did not bias our comparison of the effect of climate niche extreme
223 on tolerance traits, we aggregated CHELSA at the resolution of ERA5-land.

224 For each species, we determined whether the presence/absence EuForest dataset captured its distribution
225 limit at the dry or cold margin ~~using the expert-based EuForgen distribution. To do this, we checked~~
226 ~~whether Euforest points falling outside the EuForgen distribution had more extreme climates than points~~
227 ~~inside the EuFogen distribution.~~ For instance, EuForest captures the dry margin of a species if it in-
228 cludes absence observations in dryer locations than the margin of the species. If this is not the case, it is
229 not possible to tell whether the dry margin in EuForest data is an environmental margin or the limit of
230 the dataset. We tested the coverage of each margin by comparing the 95th percentile of *pet* and the 5th
231 percentile of *mat* between the presence and absence of each species (see details in SI5). We tested the
232 drop in the probability of presence only for the margins covered by the EuForest data.

233

234 **Interspecific variation in species climatic niche extremes and their physiological tolerance**
235 **traits**

236 For each of the five climatic variables (*map*, *mat*, *pet*, T_{min} and Ψ_{min}) and each species, we computed
237 its respective extreme (hereafter called climatic niche extremes) as the 5th percentile for *map*, *mat*, T_{min}
238 and Ψ_{min} or the 95th percentile for *pet* over its distribution.

239 To test our first hypothesis that maximum experienced frost and drought stress explain interspecific vari-
240 ation in LT_{50} and Ψ_{50} better than classical climatic variables, we performed univariate linear regression
241 of LT_{50} with climatic niche extremes of *mat* or T_{min} and of Ψ_{crit} with the climatic niche extremes of *map*,
242 *pet*, or Ψ_{min} . We used t-tests to test whether the regression coefficients were significantly non-null. R^2 of
243 the regression and effect-size (computed as standardised coefficients, see Schielzeth, 2010) were used to

²⁴⁴ quantify the strength of the relation between climatic niche extremes and species physiological tolerance
²⁴⁵ traits.

²⁴⁶ Distribution models and safety margins

²⁴⁷ Species-specific distribution models

²⁴⁸ Species j presence/absence in each 1x1km grid cell i was modelled assuming a Bernoulli distribution with
²⁴⁹ a probability of presence $p_{i,j}$.

²⁵⁰ We modelled $p_{i,j}$ as being limited by both safety margins with logistic functions to allow for a
²⁵¹ drastic drop in probability of presence at low safety margins. The shape of the model itself tests the
²⁵² relevance of the zero safety margin threshold. To represent that a high probability of presence occurs
²⁵³ only in areas where neither frost nor drought is limiting, we formulated the model as a multiplicative
²⁵⁴ function of the two logistic functions as:

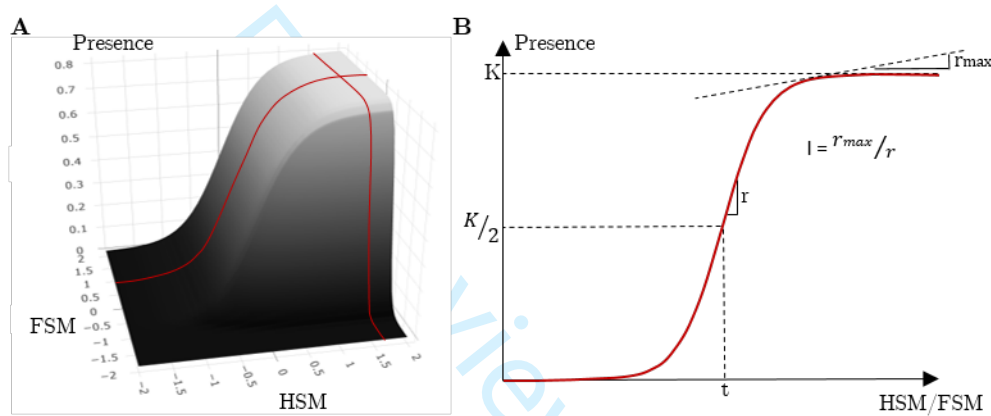
$$p_{i,j} = \frac{K_j}{[1 + \exp(-r_{FSM,j} \cdot (FSM[i,j] - t_{FSM,j}))] \cdot [1 + \exp(-r_{HSM,j} \cdot (HSM[i,j] - t_{HSM,j}))]} \quad (6)$$

²⁵⁵ with $t_{FSM,j}$, $r_{FSM,j}$ and K_j being model estimated parameters, j the species and i a grid cell. The t
²⁵⁶ parameters correspond to an offset on the safety margins and its value is key to testing the relevance of
²⁵⁷ physiological tolerance trait. If negative, the species can tolerate physiological stress and is present even
²⁵⁸ with negative safety margins (Fig. 1). If positive, the species probability of presence starts to decrease
²⁵⁹ even when safety margins are positive. The t parameters were constrained to the observed interval of
²⁶⁰ the corresponding safety margins, and we assumed a normal prior centred around 0 with a standard
²⁶¹ deviation of 1. The r parameters correspond to the slope at the inflection point at the threshold t . The
²⁶² larger r , the more sensitive the species is to its margin of safety. The r parameters were restricted to
²⁶³ positive values to force safety margins to have a positive link with higher presence rates or no effect. $\overline{K_{sp}}$
²⁶⁴ K_j is the maximum probability of presence when both safety margins are favourable to the species. The
²⁶⁵ $\overline{K_{sp}} K_j$ parameters are inherently between 0 and 1, and a normal distribution prior was set. We used an
²⁶⁶ informative prior for the mean based on the mean probability of presence of the species in its EuForGen
²⁶⁷ distribution and a standard deviation of 1.

²⁶⁸ We also explored alternative simpler models where the probability of presence p_i is related only to

269 *HSM*, or to *FSM*, or none (see equations in SI6).

270 For each species, we only fitted models that included the safety margins for which the EuForest data
 271 covered their respective climatic margins (*FSM* for cold margin and *HSM* for dry margin). In other
 272 words, for a species for which no absence data could cover the cold limit, we did not fit a model that
 273 included the *FSM*. Models were inferred using the Bayesian statistical paradigm with the Rstan package
 274 (Carpenter et al., 2017). All other statistical analyses were performed using R software (R Core Team,
 275 2022).



276 Figure 1: Logistic model for the probability of species presence. A. The probability of presence is represented
 as a bivariate function of *FSM* and *HSM*. If one of the two safety margins is limiting, the probability of presence drops.
 B. The red transects in A are plotted in one dimension with key parameters of the model. The inflection index I and its
 calculation are also shown.

276 Model selection and index

277 We first discarded models with poor convergence based on two criteria: more than 1% of divergent transi-
 278 tions during sampling of the four chains and potential scale reduction factor - $RHat > 1.1$ (Gelman et al.,
 279 2013). Then, for each species, we selected the model with the lowest Bayesian Information Criterion -
 280 BIC (Schwarz, 1978) ~~-among the converging models. The difference in BIC with the next best model~~
 281 ~~was always greater than 2 indicating strong support for the selected model (see Table S5).~~

282

283 We computed AUC (Fielding and Bell, 1997) for each model using the model predictions over the
 284 data used in the fit. AUC measures the fit quality, 0.5 being the AUC of a random model and 1 of a
 285 perfect fit.

286 We calculated an inflection index I to assess the strength of the drop of the species probability of
 287 presence along FSM or HSM, based on the ratio between the slope at the 95th percentile of the safety
 288 margin and the slope at the inflection point (r). The inflection index was one minus the ratio and ranged
 289 between 0 and 100%. The higher I , the more non-linear the model (Fig. 1). To facilitate the comparison
 290 of t_{hsm} and t_{fsm} , we derived rescaled thresholds. We scaled the t parameters to the range of safety
 291 margins covered by each species.

292 **Transferability of generic safety margins-based to "unobserved species"**

293 Because safety-margin-based distribution models incorporate species-specific physiological tolerance traits,
 294 they should have a good ability to predict species for which no occurrence observations were used in the
 295 fit ('unobserved species'). To assess transferability, we repeatedly calibrated a generic model on all species
 296 except one and predicted the distribution of this "unobserved" species with the corresponding model (in
 297 total we fitted 38 generic models). For the generic models we use the same structure as equation 6 but
 298 with a random species effect on the asymptote $K_{sp} - K_j$ (assuming a beta distribution), to account for
 299 differences between species, as:

$$p_{i,j} = \frac{K_j}{[1 + \exp(-r_{FSM} \cdot (FSM[i,j] - t_{FSM}))] \cdot [1 + \exp(-r_{HSM} \cdot (HSM[i,j] - t_{HSM}))]} \quad (7)$$

$$K_j \sim \mathcal{B}(\lambda \cdot K, \lambda \cdot (1 - K)) \quad (8)$$

300 with t_{FSM} , r_{FSM} , K_j , K being the and λ being model estimated parameters, j being the species and
 301 i the grid cell. K being the mean random asymptote of all species, λ a shape parameter, and r and t are
 302 common to all species (see SI7 for model details). We assessed the ability of a generic model to predict
 303 the distribution of an unobserved species using the True Skill Statistic (TSS) (Allouche et al., 2006) and
 304 the average AUC over all unobserved species (Fielding and Bell, 1997). Higher TSS and AUC closer to
 305 1 indicates a better prediction quality. We used only 31 generic models because the other 7 models led
 306 to convergence issues.

307 **~~Effect of local light competitive hierarchy on sensitivity to safety margins~~**

308 For each species, we extracted an index of shade tolerance from . Shade tolerance ranges from 0 to
309 5, from the less to the more shade-tolerant species. We used the shade tolerance index as an index
310 of species' position in the competitive hierarchy for light and computed a light competitive dominance
311 index corresponding to the mean number of more shade tolerant species occurring simultaneously with
312 the target species. The higher the competitive dominance index, the more the species is exposed to the
313 competitive effect of superior species. To test our fourth hypothesis, we performed a linear regression
314 between species-specific model outputs (I and t of *HSM* and *FSM*) and the light competitive dominance
315 index. We used t-tests to test whether the regression coefficients were significantly non-null.

316 Results

317 Frost and drought tolerance traits are strongly correlated with maximum ex- 318 perienced stresses

319 We found that frost and drought tolerance traits (Ψ_{crit} and LT_{50}) were correlated with climatic niche
320 extremes based on physiological stress, the effects being equal or slightly stronger than for climatic niche
321 extremes based on classical climatic variables. For Ψ_{crit} , we observed that the minimum soil potential
322 extreme (i.e. 5th percentile of Ψ_{min}) has the strongest effect (standardised regression coefficient and its
323 95% confidence interval: 0.77 [0.29,1.24]; $p = 2.60e-3$; $p < 0.01$; Fig. 2). This suggests that trees have
324 lower Ψ_{crit} , thus higher resistance to xylem embolism, when their niches extend into extremely low soil
325 moisture. Potential evapotranspiration extremes pet also correlated with Ψ_{crit} , with higher pet correlated
326 with more resistant species. Finally, we found that low precipitation extremes had no correlation with
327 Ψ_{crit} . We also tested the effect of $map - pet$, which is a classical aridity index, but found no effect.

328 We For LT_{50} , we observed an equivalent effect of extreme low temperature (i.e. 5th percentile of T_{min} ;
329 0.51 [0.31,0.71]; Fig. 2) and extreme mean annual temperature (i.e. 5th percentile of mat ; 0.56[0.33,0.80];
330 Fig. 2). This led to lower LT_{50} with decreasing T_{min} and mat . These effects were both significant and
331 positive ($p = 1.00e-5$ and $p = 2.06e-5$ for $p < 0.001$ for both T_{min} and mat respectively).

332 We also investigated correlations between all the climatic niche extremes and found correlations greater
333 than 0.9 between Ψ_{min} and pet , and between T_{min} and mat (see details in Fig. S7)

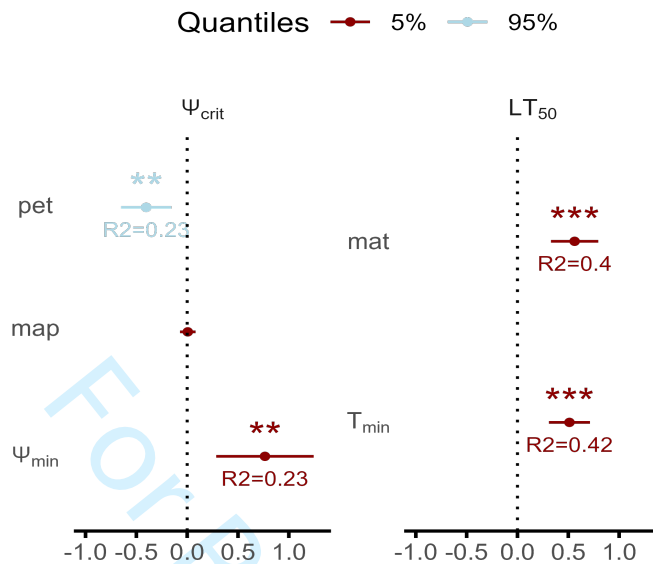


Figure 2: Standardized coefficients of the regression of physiological tolerance traits against climatic niche extremes. The climatic niche extreme is estimated using climatic variables (5^{th} percentile of mean annual precipitation map and mean annual temperature mat , 95^{th} percentile of annual potential evapotranspiration pet) or maximum experienced stress (5^{th} percentile of minimum temperature T_{min} and minimum soil potential Ψ_{min}). Ψ_{crit} refers to Ψ_{50} (gymnosperms) or Ψ_{88} (angiosperms). The analysis includes all species for which the occurrence data cover the corresponding margin of the distribution (see Methods for details). *, ** and *** indicate a significant relationship with p-values less than 0.05, 0.01 and 0.001 respectively. Bars indicate 95% confidence intervals.

³³⁴ Safety margins explain drops in species probability of presence are
³³⁵ related to their safety margins

³³⁶ Our results show that for species for which occurrence data covered their frost or drought margin, the
³³⁷ corresponding safety margin was generally selected in models over the null model.
³³⁸ In particular, among the 30 species that had absence/presence distribution data that allowed us to test
³³⁹ the effect of *FSM*, 26 had *FSM* selected in the final model. Similarly, among the 28 species that had
³⁴⁰ absence/presence distribution data that allowed us to test the effect of *HSM*, all of them had *HSM*
³⁴¹ selected in the final model. Within these two groups of species, we tested both safety margins for 23
³⁴² species and found that 19 of them were indeed explained by both *FSM* and *HSM*. Out of the 38 species,
³⁴³ the distribution of only three species could not be explained by their safety margins (*Juniperus communis*,
³⁴⁴ *Populus alba* and *Quercus pubescens*). The mean AUC of all models was 0.69, with 25 species having
³⁴⁵ AUC over 0.65 indicating acceptable fits, and six of which had particularly good fits with AUC over 0.8.
³⁴⁶ The ten other species had low AUC (<0.65) which may be caused by their very low prevalence (median

347 prevalence and quartiles of these 10 species: 0.017 [0.013,0.04]; of the 25 other species: 0.11 [0.04,0.22]).

348 **Species probability of presence respond non-linearly to their safety margin**

349 We observed that crossing the LT_{50} thresholds resulted in a drastic drop in the probability of presence,
350 while the decrease was more progressive for Ψ_{50} . The rescaled thresholds of *FSM* (mean estimate of
351 rescaled t with its 95% confidence interval: 0.04 [-0.01,0.10]) were on average closer to zero than those of
352 *HSM* (mean estimate of rescaled t with its 95% confidence interval 0.14 [0.01,0.27], Fig. 3B). This means
353 that the probability of species presence drops close to the point where the species frost tolerance LT_{50} is
354 exceeded, while the thresholds for *HSM* are higher with wide confidence intervals. This large variability
355 is mainly due to the angiosperm species. Moreover, the *HSM* thresholds of angiosperms are three times
356 lower than those of gymnosperms, indicating a drop in the probability of presence closer to the point
357 where the species' drought tolerance is crossed.

358 The inflection index I for *FSM* (Fig. 3B) was 10 times higher than for *HSM*, showing a stronger
359 non-linearity compared to *FSM*/*HSM* (Fig. 3A).

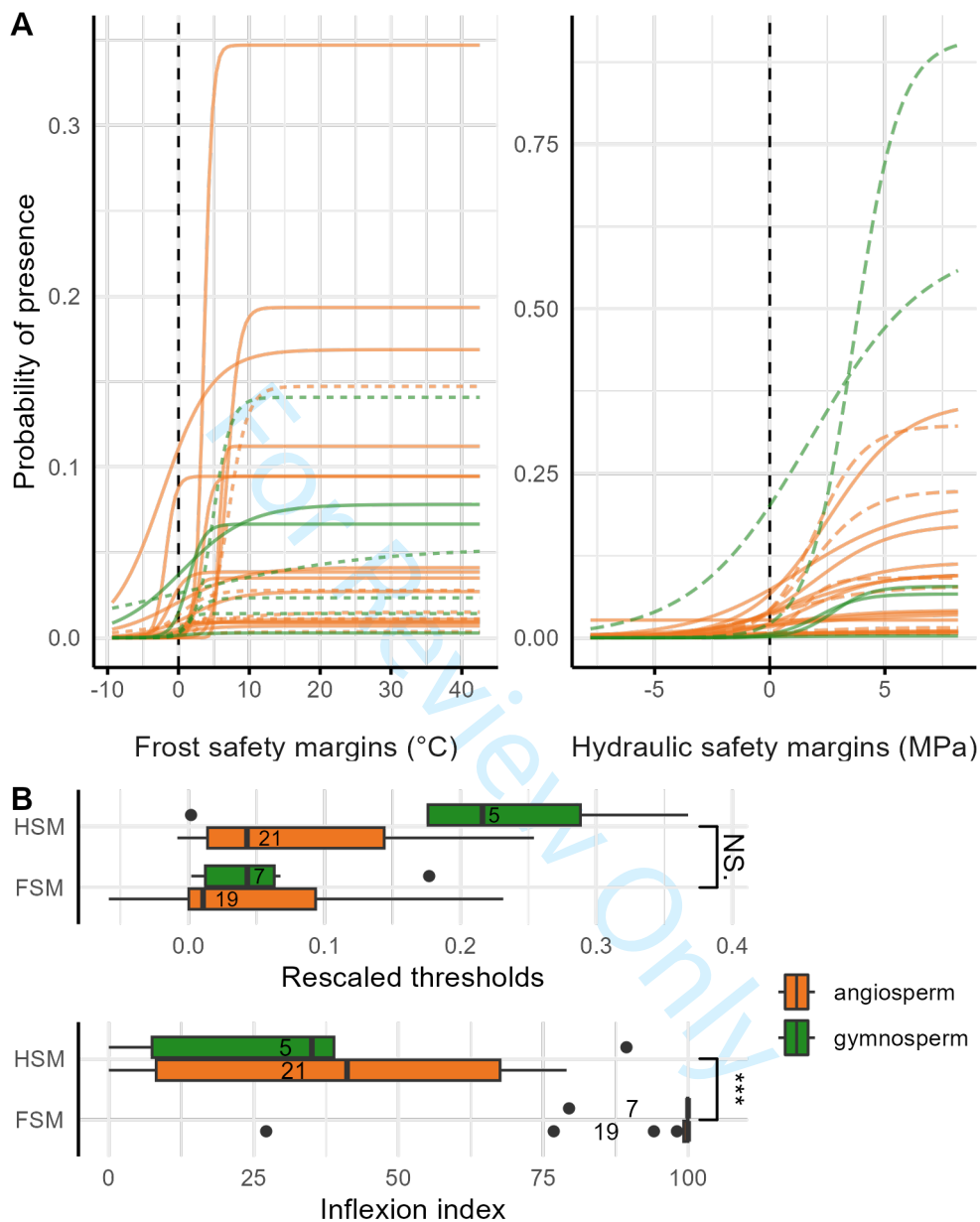


Figure 3: Predicted probability of presence as a function of *FSM* and *HSM* (A) and parameters of the function describing the shift in probability of presence - the rescaled threshold t and the inflection index I . (B). A. Predictions are made from the mean model outputs, with the other safety margins fixed at their 95th percentiles. Colours highlight differences between angiosperms (orange) and gymnosperms (green). Dashed lines represent species with a model including only one safety margin. B. Metrics of the model: thresholds t rescaled by the range of safety margin for the species, and the inflection index I calculated as the ratio between the slope r at the inflection point t and at 95th percentiles of the safety margin range. The number of species in each distribution is shown in the box plots. Differences between groups, i.e. *HSM* vs. *FSM*, were tested by t-test and, if significant, are indicated by *, ** or ***, corresponding to p-values less than 0.05, 0.01 and 0.001, respectively.

360 Transferability of safety margin model for species without occurrence data

361 With a generic model based on safety margins, we found ~~good-moderate~~ predictive ability for a species
362 not included in the model fit, *i.e.* "unobserved species". The mean AUC of predictions for each species
363 was 0.67, with an inter-quartile range of 0.63-0.72. Only five species had an AUC below 0.6. This was
364 close to AUC found for traits-SDM models (AUC median and inter-quartile of Vesk et al. (2021) : 0.65
365 [0.57,0.77]). The TSS also indicated good fit quality, with a mean TSS of 0.30 and an inter-quartile range
366 of 0.23-0.40 (see Table S7).

367 ~~How does light competitive dominance index affect the link between probability 368 of presence and safety margin?~~

369 ~~We assumed that species with a low light competitive dominance index would have a steeper and more
370 non-linear decline in the probability of presence for both safety margins (*i.e.* high I) than species with a
371 high light competitive dominance index. Indeed, these species would not be limited by light competition
372 and abiotic physiological stress tolerance would be the primary limitation of the species. Yet we did not
373 find any significant effect of the light competitive dominance index on I nor t (see SI). In addition, the
374 sensitivity of the models was on average higher than their specificity (mean sensitivity and inter-quartile:
375 0.83 [0.79,0.90], specificity: 0.47 [0.39,0.58]), indicating a pattern of over-predicting presence over absence.~~

376 Discussion

377 Our attempt to combine frost and drought safety margins in correlative species distribution models showed
378 that for 35 European tree species the probability of presence dropped when their tolerance thresholds were
379 exceeded. In particular, the cold limit was close to a zero safety margin and corresponded to a strongly
380 non-linear decrease in the probability of presence, whereas the probability of presence started to decrease
381 more progressively at positive drought safety margins. Our model represents a new approach to including
382 traits in SDMs, and demonstrates the relevance of physiological tolerance traits and safety margins to
383 model species distribution. Interestingly, our correlative model based on safety margins performed well at
384 predicting "unobserved species", with prediction metrics being of the same order as previous traits-SDM.

385 Maximum experienced stresses explain inter-specific variability in physiologi-
386 cal tolerance traits

387 Interspecific variations in frost and drought tolerance traits were explained by niche climatic extremes,
388 and in particular by maximum experienced stress (Fig. 2). We found higher or equivalent correlations
389 effect-size between LT_{50} and Ψ_{50} and the extremes of their respective maximum experienced stress T_{min}
390 and Ψ_{min} than with the more classical climatic variables *map*, *pet* and *mat*. Our results support our
391 initial hypothesis that the maximum experienced stresses are closely related to the physiological limits
392 of the species, despite the uncertainty in the calculation of maximum drought stress. This is consistent
393 with recent studies that have emphasised the importance of using climatic extremes rather than averages
394 to explain ecological patterns, despite being well correlated (Stewart et al., 2021). Moreover, this agrees
395 with Blackman et al. (2012) and Brodribb et al. (2014) who also showed this pattern when looking at
396 correlation of Ψ_{50} with the 5th percentile of *map* or the driest quarter rainfall. Larter et al. (2017) and
397 Skelton et al. (2021) reported that species with lower mean *map* were found to have greater resistance
398 to embolism, whereas we found no correlation significant relationship between Ψ_{50} and *map* percentiles.
399 This could be because, unlike the above studies, we did not cover very arid environments. Other more
400 complex variables (such as the precipitation in the driest months) could also have been tested to explain
401 variations in Ψ_{50} , but here we focused on the most classical variables.

402 Fewer studies have investigated the environmental variability of species' frost tolerance traits. In particu-
403 lar, they have shown associations between cold stress resistance and niche minimum temperature (Zanne
404 et al., 2018), potential elevation limits (Charrier et al., 2013), niche mean temperature and precipitation
405 (Kreyling et al., 2015). In addition, Lancaster and Humphreys (2020) found a latitudinal cline for frost
406 tolerance in different plant groups. A key advance of our study is to show that winter maximum frost
407 hardiness is useful to standardise LT_{50} extracted from the literature for numerous species and capture
408 species' distribution low-temperature limit.

409 Safety margins are relevant for explaining drop in species probability of pres-
410 ence

411 *Differential sensitivity to frost and drought.* Our analysis showed that species' probability of presence
412 dropped before they reached their stress tolerance. In addition, crossing the frost tolerance threshold,

413 LT_{50} , resulted in a steeper decrease in the probability of presence than for the drought threshold (Fig.
414 3).

415 Trees' responses to their frost safety margins indicate that they often operate close to their limits in terms
416 of frost-induced cell damage during winter. This observation challenges previous studies that suggest trees
417 have broad safety margins in winter (Körner et al., 2016). However, since our model is correlative, it does
418 not demonstrate that winter frost-induced damage is the driving mechanism behind the cold range limits
419 of species. Many other mechanisms could explain the cold range limits of species, such as embolisms
420 caused by freeze-thaw cycles or late frosts damaging, late frosts that damage reproductive tissues or
421 reducing the growing season shorten growing season. (Charrier et al., 2017; Morin et al., 2007; Zanne
422 et al., 2018). Winter LT_{50} could be indirectly correlated with these other frost-related limiting factors.
423 Nevertheless, winter LT_{50} seems a relevant trait to capture interspecific variability in frost tolerance in a
424 standardised way and is valuable for understanding species distributions.

425 The response to drought safety margins was less clear: thresholds were on average higher than zero, and
426 non-linearity indices indicated a more progressive effect than for frost. Moreover, the drop in the proba-
427 bility of presence was closer to the point where the species' drought tolerance is crossed for angiosperms
428 than for gymnosperms. This pattern arises even though we used different Ψ_{crit} for angiosperms and
429 gymnosperms to account for the anatomical and physiological differences between the two groups (Ψ_{88}
430 for angiosperms and Ψ_{50} for gymnosperms). Previous studies have already shown that gymnosperms op-
431 erate at greater hydraulic safety margins than angiosperms, highlighting the need for separate analyses of
432 their drought resistance (Choat et al., 2012; Urli et al., 2013). This may explain the observed taxonomic
433 differences.

434 The positive threshold and low non-linearity suggest that it is challenging to capture drought vulnera-
435 bility in a single dimension. In fact, there are many different drought resistance strategies (Choat et al.,
436 2018; Martin-StPaul et al., 2017). For example, in addition to embolism resistance, stomatal regulation
437 is critical in controlling tree drought survival. Stomatal closure significantly reduces water loss, and
438 the timing of this closure varies greatly between species, typically preceding extensive xylem embolism
439 (Martin-StPaul et al., 2017). Residual water loss through leaf cuticle, bark and 'leaky' closed stomata
440 also plays a key role in determining the timing of plant death during drought (Martin-StPaul et al., 2017).
441 Leaf shedding could mitigate water loss during drought and allow angiosperms to reduce investment in
442 xylem embolism resistance. Root function and its ability to disconnect from the soil may also play a

critical role in some species. Furthermore, increased pathogen susceptibility during drought adds another layer of complexity to the situation (Trugman et al., 2021). In addition, unlike frost, drought is associated with water, a shared resource for which multiple species compete directly. The weaker effect of drought in our distribution models could also result from higher uncertainties in our metric of maximum drought stress compared to our metric of maximum frost stress. Indeed, soil water content is notoriously more difficult to estimate in climate reanalysis than temperature (Muñoz-Sabater et al., 2021; Velikou et al., 2022).

Yet, this differential response of probability of presence to frost and drought echoes studies comparing the role of frost versus heat tolerance. Araújo et al. (2013) and Lancaster and Humphreys (2020) highlighted greater variability in frost tolerance between lineages and a better link to species' latitudinal limits than for heat tolerance.

Distribution modelling at the interface between correlative and mechanistic models. We found that the distribution of most of our 38 species was related to their safety margins. Only the distribution of three species, *Juniperus communis*, *Populus alba* and *Quercus pubescens*, could not be explained by any of the safety margins.

Our model allowed us to introduce information from physiological traits into a correlative distribution model while maintaining a simplistic approach. As advocated in the review by Dormann et al. (2012), there is an urgent need to incorporate more physiology into correlative models. This is because mechanistic models perform better in novel climatic regimes and for species with limited occurrence data, whereas correlative models are more easily transferable across space and time (Dormann et al., 2012; Higgins et al., 2020). To bridge this gap, one strategy consist in calibrating physiological mechanistic models for numerous species (Chuine and Beaubien, 2001; Martin-StPaul et al., 2017) to project species distributions forward. Mechanistic models can also be inversely calibrated from species occurrence data (Hartig et al., 2012) to more easily estimate the large number of parameters. Another strategy rooted in the correlative philosophy is to fit correlative SDMs with trait-dependant parameters (Pollock et al., 2012; Vesk et al., 2021). These traits-SDMs mostly rely on traits capturing leaf economics, establishment or competitive strategies, but ~~which~~ do not enable interpretation of model parameters in terms of physiological processes. In animal ecology, the "biophysical ecology" paradigm proposes to directly incorporate the link between functional traits and environments into SDMs, for example using as a predictor the difference between body temperature and maximum temperature (Kearney and Porter, 2009).

473 Our safety margins are the equivalent of these predictors for tree species and our model uses a similar
474 approach as "biophysical ecology", to fit a correlational distribution model in a physiological stress space
475 and account directly for the limits set by species physiological tolerance traits. This results in a simpler
476 model than physiological mechanistic models, but still allows a good connection with physiological pro-
477 cesses and good transferability to species not included in the fit and for which only physiological traits
478 information are available. Indeed, we found that when trying to predict the distribution of a species
479 without presence/absence calibration data, our generic models based on safety margins gave ~~similar AUC~~
480 ~~ranges than for AUC ranges similar to trait-SDMs . Further, the model itself tests the relevance of these~~
481 ~~traits for delimiting areas of excessive stress, and evaluates if projecting safety margins can be used as~~
482 ~~simplistic indicators of tree species' vulnerability to climate change. (AUC median and inter-quartile of~~
483 Vesk et al., 2021 : 0.65 [0.57,0.77]). It would be interesting to also test the predictive ability of our model
484 in new continents or regions with a distinct species pool as in Vesk et al. (2021). We noted an average
485 higher sensitivity of the model than specificity, highlighting the over-predicting trend of our models. This
486 might be caused by constraints that safety margins could not catch, such as higher competition in species
487 hot margins (Sexton et al., 2009).

488

489 ~~Competitive dominance index and species response to their safety margin~~

490 ~~We expected that species undergoing more competition for light would be less sensitive to their margin~~
491 ~~of safety, as they are limited by other biotic processes. However, we did not observe any effect of the~~
492 ~~light competitive dominance index. This is certainly due to the very crude index we used to test the~~
493 ~~light competitive effect. Estimating the competitive effect on tree species distribution would probably~~
494 ~~require more than just static presence-absence data (data on population dynamic or experimental data,~~
495 ~~Lyu and Alexander, 2022). The challenge of our safety margin approach is to find a good compromise~~
496 ~~in the simplification of physiological processes. Too much detail would lead to the complexity pitfalls~~
497 ~~of mechanistic models, while too much simplicity would produce indicators that are too coarse. For~~
498 ~~instance, it would be interesting to account for the duration and frequency of negative safety margins.~~
499 ~~The duration of drought stress is indeed important (Martin-StPaul et al., 2017), but remains difficult to~~
500 ~~include in safety margins.~~

501 Limitations of our study

502 Due to limited data availability, we did not consider intra-specific variability in physiological tolerance
503 traits. Existing studies suggest modest intraspecific variability in LT_{50} , with populations at the cold
504 extremes of the distribution exhibiting higher resistance (Morin et al., 2007). Studies of plasticity drivers
505 of Ψ_{50} are very scarce and often focus on a few species (Anderegg, 2015; González-Muñoz et al., 2018).
506 When accounting for the high measurement errors, most studies concluded that this trait is strongly
507 conserved (Lamy et al., 2014; Skelton et al., 2019) (but see [Anderegg, 2015](#)[Anderegg \(2015\)](#)). In addition,
508 our analysis did not show a positive probability of occurrence for negative safety margins, which would
509 be expected if plasticity allows species to be more tolerant in extreme environments.
510 Second, by choosing tolerance thresholds related to species survival, we assumed that species distribution
511 is limited by this demographic process. However, numerous studies (Hargreaves et al., 2014; Sexton et al.,
512 2009) have shown that distribution also depends on growth and reproduction. These complex mechanisms
513 remain difficult to capture with physiological stress tolerance traits. Finally, our soil potentials map
514 depends on the 9x9 km soil water content map, which is very crude to capture such a highly heterogeneous
515 variable.

516 Conclusion

517 Our study is an important step towards building correlative models that are better constrained by phys-
518 iological traits. The originality lies in modeling species distribution using physiological safety margins,
519 derived from European climate reanalysis and frost and drought tolerance traits. It is a complementary
520 approach to trait-SDMs, bridging the gap between correlative and mechanistic models. [This paves the](#)
521 [way to estimate](#) Our frost and drought safety margins pave the way for delimiting areas of tree species'
522 [vulnerability](#) ranges that are vulnerable to climate change[based on their safety margins](#).

523 References

- 524 Allouche, O., A. Tsoar, and R. Kadmon (2006). Assessing the accuracy of species distribution models:
525 prevalence, kappa and the true skill statistic (TSS). *Journal of Applied Ecology* 43.6, pp. 1223–1232.
526 DOI: 10.1111/j.1365-2664.2006.01214.x.
- 527 Anderegg, W. R. L. (2015). Spatial and temporal variation in plant hydraulic traits and their relevance
528 for climate change impacts on vegetation. *New Phytologist* 205.3, pp. 1008–1014. DOI: 10.1111/nph.
529 12907.
- 530 Anderegg, W. R. L., A. Flint, C. Y. Huang, L. Flint, J. A. Berry, et al. (2015). Tree mortality predicted
531 from drought-induced vascular damage. *Nature Geoscience* 8.5, pp. 367–371. DOI: 10.1038/ngeo2400.
- 532 Araújo, M. B., F. Ferri-Yáñez, F. Bozinovic, P. A. Marquet, F. Valladares, et al. (2013). Heat freezes
533 niche evolution. *Ecology Letters* 16.9. Ed. by D. Sax, pp. 1206–1219. DOI: 10.1111/ele.12155.
- 534 Benito Garzón, M., N. González Muñoz, J.-P. P. Wigneron, C. Moisy, J. Fernández-Manjarrés, et al.
535 (2018). The legacy of water deficit on populations having experienced negative hydraulic safety margin.
536 *Global Ecology and Biogeography* 27.3, pp. 346–356. DOI: 10.1111/geb.12701.
- 537 Blackman, C. J., T. J. Brodribb, and G. J. Jordan (2012). Leaf hydraulic vulnerability influences species'
538 bioclimatic limits in a diverse group of woody angiosperms. *Oecologia* 168.1, pp. 1–10. DOI: 10.1007/
539 S00442-011-2064-3/FIGURES/3.
- 540 Brodribb, T. J., S. A. McAdam, G. J. Jordan, and S. C. Martins (2014). Conifer species adapt to low-
541 rainfall climates by following one of two divergent pathways. *Proceedings of the National Academy of
542 Sciences* 111.40, pp. 14489–14493. DOI: 10.1073/pnas.1407930111.
- 543 Carpenter, B., A. Gelman, M. D. Hoffman, D. Lee, B. Goodrich, et al. (2017). Stan : A Probabilistic
544 Programming Language. *Journal of Statistical Software* 76.1. DOI: 10.18637/jss.v076.i01.
- 545 Charra-Vaskou, K., G. Charrier, R. Wortemann, B. Beikircher, H. Cochard, et al. (2012). Drought and
546 frost resistance of trees: a comparison of four species at different sites and altitudes. *Annals of Forest
547 Science* 69.3, pp. 325–333. DOI: 10.1007/s13595-011-0160-5.
- 548 Charrier, G., H. Cochard, and T. Ameglio (2013). Evaluation of the impact of frost resistances on potential
549 altitudinal limit of trees. *Tree Physiology* 33.9, pp. 891–902. DOI: 10.1093/treephys/tpt062.
- 550 Charrier, G., M. Nolf, G. Leitinger, K. Charra-Vaskou, A. Losso, et al. (2017). Monitoring of Freezing
551 Dynamics in Trees: A Simple Phase Shift Causes Complexity. *Plant Physiology* 173.4, pp. 2196–2207.
552 DOI: 10.1104/PP.16.01815.
- 553 Choat, B., T. J. Brodribb, C. R. Brodersen, R. A. Duursma, R. López, et al. (2018). Triggers of tree
554 mortality under drought. *Nature* 558.7711, pp. 531–539. DOI: 10.1038/s41586-018-0240-x.
- 555 Choat, B., S. Jansen, T. J. Brodribb, H. Cochard, S. Delzon, et al. (2012). Global convergence in the
556 vulnerability of forests to drought. *Nature* 491.7426, pp. 752–755. DOI: 10.1038/nature11688.
- 557 Chuine, I. and E. G. Beaubien (2001). Phenology is a major determinant of tree species range. *Ecology
558 Letters* 4.5, pp. 500–510. DOI: 10.1046/j.1461-0248.2001.00261.x.
- 559 Dormann, C. F., S. J. Schymanski, J. Cabral, I. Chuine, C. Graham, et al. (2012). Correlation and process
560 in species distribution models: bridging a dichotomy. *Journal of Biogeography* 39.12, pp. 2119–2131.
561 DOI: 10.1111/j.1365-2699.2011.02659.x.
- 562 Elith, J. and J. R. Leathwick (2009). Species Distribution Models: Ecological Explanation and Prediction
563 Across Space and Time. *Annual Review of Ecology, Evolution, and Systematics* 40.1, pp. 677–697.
564 DOI: 10.1146/annurev.ecolsys.110308.120159.
- 565 Fielding, A. H. and J. F. Bell (1997). A review of methods for the assessment of prediction errors in
566 conservation presence/absence models. *Environmental Conservation* 24.1, pp. 38–49. DOI: 10.1017/
567 S0376892997000088.
- 568 Gelman, A., J. B. Carlin, H. S. Stern, D. B. Dunson, A. Vehtari, et al. (2013). *Bayesian Data Analysis,
569 Third Edition*. CRC Press, p. 677.

- 570 González-Muñoz, N., F. Sterck, J. M. Torres-Ruiz, G. Petit, H. Cochard, et al. (2018). Quantifying in situ
571 phenotypic variability in the hydraulic properties of four tree species across their distribution range
572 in Europe. *PLOS ONE* 13.5. Ed. by B. Heinze, e0196075. DOI: 10.1371/journal.pone.0196075.
- 573 Hammond, W., B. Choat, D. Johnson, M. Ali Ahmed, L. Anderegg, et al. (2021). "The global vulnerability
574 of plant xylem". In: *AGU FM*. Vol. 2021, B31F-07.
- 575 Hargreaves, A. L., K. E. Samis, and C. G. Eckert (2014). Are Species' Range Limits Simply Niche Limits
576 Writ Large? A Review of Transplant Experiments beyond the Range. *The American Naturalist* 183.2,
577 pp. 157–173. DOI: 10.1086/674525.
- 578 Hartig, F., J. Dyke, T. Hickler, S. I. Higgins, R. B. O'Hara, et al. (2012). Connecting dynamic vegetation
579 models to data - an inverse perspective. *Journal of Biogeography* 39.12, pp. 2240–2252. DOI: 10.1111/
580 j.1365-2699.2012.02745.x.
- 581 Hiederer, R. (2013). *Mapping Soil Properties for Europe - Spatial Representation of Soil Database At-*
582 *tributes*, p. 47.
- 583 Higgins, S. I., M. J. Larcombe, N. J. Beeton, T. Conradi, and H. Nottebrock (2020). Predictive ability of a
584 process-based versus a correlative species distribution model. *Ecology and Evolution* 10.20, pp. 11043–
585 11054. DOI: 10.1002/ece3.6712.
- 586 Karger, D. N., O. Conrad, J. Böhner, T. Kawohl, H. Kreft, et al. (2017). Climatologies at high resolution
587 for the earth's land surface areas. *Scientific Data* 4.1, pp. 1–20. DOI: 10.1038/sdata.2017.122.
- 588 Kearney, M. and W. Porter (2009). Mechanistic niche modelling: combining physiological and spatial
589 data to predict species' ranges. *Ecology Letters* 12.4, pp. 334–350. DOI: 10.1111/j.1461-0248.2008.
590 01277.x.
- 591 Körner, C., D. Basler, G. Hoch, C. Kollas, A. Lenz, et al. (2016). Where, why and how? Explaining the
592 low-temperature range limits of temperate tree species. *Journal of Ecology* 104.4. Ed. by M. Turnbull,
593 pp. 1076–1088. DOI: 10.1111/1365-2745.12574.
- 594 Kreyling, J., S. Schmid, and G. Aas (2015). Cold tolerance of tree species is related to the climate of their
595 native ranges. *Journal of Biogeography* 42.1. Ed. by S. Higgins, pp. 156–166. DOI: 10.1111/jbi.12411.
- 596 Lamy, J.-B., S. Delzon, P. S. Bouche, R. Alia, G. G. Vendramin, et al. (2014). Limited genetic variability
597 and phenotypic plasticity detected for cavitation resistance in a Mediterranean pine. *New Phytologist*
598 201.3, pp. 874–886. DOI: 10.1111/nph.12556.
- 599 Lancaster, L. T. and A. M. Humphreys (2020). Global variation in the thermal tolerances of plants.
600 *Proceedings of the National Academy of Sciences* 117.24, pp. 13580–13587. DOI: 10.1073/pnas.
601 1918162117.
- 602 Larter, M., S. Pfautsch, J.-C. Domec, S. Trueba, N. Nagalingum, et al. (2017). Aridity drove the evolution
603 of extreme embolism resistance and the radiation of conifer genus *Callitris*. *New Phytologist* 215.1,
604 pp. 97–112. DOI: 10.1111/nph.14545.
- 605 Lenz, A., G. Hoch, Y. Vitasse, and C. Körner (2013). European deciduous trees exhibit similar safety
606 margins against damage by spring freeze events along elevational gradients. *New Phytologist* 200.4,
607 pp. 1166–1175. DOI: 10.1111/nph.12452.
- 608 Lindner, M., J. B. Fitzgerald, N. E. Zimmermann, C. Reyer, S. Delzon, et al. (2014). Climate change
609 and European forests: What do we know, what are the uncertainties, and what are the implications
610 for forest management? *Journal of Environmental Management* 146, pp. 69–83. DOI: 10.1016/j.jenvman.
611 2014.07.030.
- 612 Lindström, A., E. Stattin, D. Gräns, and E. Wallin (2014). Storability measures of Norway spruce and
613 Scots pine seedlings and assessment of post-storage vitality by measuring shoot electrolyte leakage.
614 *Scandinavian Journal of Forest Research* 29.8, pp. 717–724. DOI: 10.1080/02827581.2014.977340.
- 615 Lyu, S. and J. M. Alexander (2022). Competition contributes to both warm and cool range edges. *Nature*
616 *Communications* 13.1, p. 2502. DOI: 10.1038/s41467-022-30013-3.

- 617 Mantova, M., S. Delzon, C. M. Rodriguez-dominguez, M. A. Ahmed, S. Trueba, et al. (2022). On the path
618 from xylem hydraulic failure to downstream cell death. *New Phytologist*, pp. 1–14. DOI: 10.1111/
619 nph.18578.
- 620 Martin-StPaul, N., S. Delzon, and H. Cochard (2017). Plant resistance to drought depends on timely
621 stomatal closure. *Ecology Letters* 20.11. Ed. by H. Maherli, pp. 1437–1447. DOI: 10.1111/ele.12851.
- 622 Martínez-Vilalta, J., L. S. Santiago, R. Poyatos, L. Badiella, M. Cáceres, et al. (2021). Towards a statisti-
623 cally robust determination of minimum water potential and hydraulic risk in plants. *New Phytologist*
624 232.1, pp. 404–417. DOI: 10.1111/nph.17571.
- 625 Mauri, A., G. Strona, and J. San-Miguel-Ayanz (2017). EU-Forest, a high-resolution tree occurrence
626 dataset for Europe. *Scientific Data* 4.1, p. 160123. DOI: 10.1038/sdata.2016.123.
- 627 Morin, X., T. Ameglio, R. Ahas, C. Kurz-Besson, V. Lanta, et al. (2007). Variation in cold hardiness
628 and carbohydrate concentration from dormancy induction to bud burst among provenances of three
629 European oak species. *Tree Physiology* 27.6, pp. 817–825. DOI: 10.1093/treephys/27.6.817.
- 630 Muñoz-Sabater, J., E. Dutra, A. Agustí-Panareda, C. Albergel, G. Arduini, et al. (2021). ERA5-Land:
631 a state-of-the-art global reanalysis dataset for land applications. *Earth System Science Data* 13.9,
632 pp. 4349–4383. DOI: 10.5194/essd-13-4349-2021.
- 633 Nguyen, D. and B. Leung (2022). How well do species distribution models predict occurrences in exotic
634 ranges? *Global Ecology and Biogeography* 31.6, pp. 1051–1065. DOI: 10.1111/geb.13482.
- 635 Pollock, L. J., W. K. Morris, P. A. Vesk, L. J. Pollock, W. K. Morris, et al. (2012). The role of functional
636 traits in species distributions revealed through a hierarchical model. *Ecography* 35.8, pp. 716–725.
637 DOI: 10.1111/j.1600-0587.2011.07085.x.
- 638 R Core Team (2022). *R: A Language and Environment for Statistical Computing*. R Foundation for
639 Statistical Computing, Vienna, Austria.
- 640 Ruffault, J., F. Pimont, H. Cochard, J.-L. Dupuy, and N. Martin-StPaul (2022). SurEau-Ecos v2.0: a
641 trait-based plant hydraulics model for simulations of plant water status and drought-induced mortality
642 at the ecosystem level. *Geoscientific Model Development* 15.14, pp. 5593–5626. DOI: 10.5194/gmd-
643 15-5593-2022.
- 644 Sakai, A. and W. Larcher (1987). *Mechanisms of Frost Survival*, pp. 59–96. DOI: 10.1007/978-3-642-
645 71745-1_4.
- 646 Sanchez-Martinez, P., M. Mencuccini, R. García-Valdés, W. M. Hammond, J. M. Serra-Diaz, et al. (2023).
647 Increased hydraulic risk in assemblages of woody plant species predicts spatial patterns of drought-
648 induced mortality. *Nature Ecology & Evolution* 7.10, pp. 1620–1632. DOI: 10.1038/s41559-023-
649 02180-z.
- 650 Sanchez-Martinez, P., J. Martínez-Vilalta, K. G. Dexter, R. A. Segovia, and M. Mencuccini (2020).
651 Adaptation and coordinated evolution of plant hydraulic traits. *Ecology Letters* 23.11. Ed. by E.
652 Cleland, pp. 1599–1610. DOI: 10.1111/ele.13584.
- 653 Schielzeth, H. (2010). Simple means to improve the interpretability of regression coefficients. *Methods in
654 Ecology and Evolution* 1.2, pp. 103–113. DOI: 10.1111/j.2041-210X.2010.00012.x.
- 655 Schwarz, G. (1978). Estimating the Dimension of a Model. *The Annals of Statistics* 6.2, pp. 461–464.
656 DOI: 10.1214/aos/1176344136.
- 657 Sexton, J. P., P. J. McIntyre, A. L. Angert, and K. J. Rice (2009). Evolution and ecology of species
658 range limits. *Annual Review of Ecology, Evolution, and Systematics* 40, pp. 415–436. DOI: 10.1146/
659 annurev.ecolsys.110308.120317.
- 660 Skelton, R. P., L. D. Anderegg, J. Diaz, M. M. Kling, P. Papper, et al. (2021). Evolutionary relation-
661 ships between drought-related traits and climate shape large hydraulic safety margins in western
662 North American oaks. *Proceedings of the National Academy of Sciences* 118.10. DOI: 10.1073/pnas.
663 2008987118.

- 664 Skelton, R. P., L. D. Anderegg, P. Papper, E. Reich, T. E. Dawson, et al. (2019). No local adaptation
665 in leaf or stem xylem vulnerability to embolism, but consistent vulnerability segmentation in a North
666 American oak. *New Phytologist* 223.3, pp. 1296–1306. DOI: 10.1111/nph.15886.
- 667 Stewart, S. B., J. Elith, M. Fedrigo, S. Kasel, S. H. Roxburgh, et al. (2021). Climate extreme variables
668 generated using monthly time-series data improve predicted distributions of plant species. *Ecography*
669 44.4, pp. 626–639. DOI: 10.1111/ecog.05253.
- 670 Timmis, R., J. Flewelling, and C. Talbert (1994). Frost injury prediction model for Douglas-fir seedlings in
671 the Pacific Northwest. *Tree Physiology* 14.7-9, pp. 855–869. DOI: 10.1093/treephys/14.7-9.855.
- 672 Tóth, B., M. Weynans, L. Pásztor, and T. Hengl (2017). 3D soil hydraulic database of Europe at 250 m
673 resolution. *Hydrological Processes* 31.14, pp. 2662–2666. DOI: 10.1002/HYP.11203.
- 674 Trugman, A. T., L. D. Anderegg, W. R. L. Anderegg, A. J. Das, and N. L. Stephenson (2021). Why is
675 Tree Drought Mortality so Hard to Predict? *Trends in Ecology and Evolution* 36.6, pp. 520–532. DOI:
676 10.1016/j.tree.2021.02.001.
- 677 Urli, M., A. J. Porte, H. Cochard, Y. Guengant, R. Burlett, et al. (2013). Xylem embolism threshold for
678 catastrophic hydraulic failure in angiosperm trees. *Tree Physiology* 33.7, pp. 672–683. DOI: 10.1093/
679 treephys/tpt030.
- 680 Van Genuchten, M. T. (1980). A Closed-form Equation for Predicting the Hydraulic Conductivity of
681 Unsaturated Soils. *Soil science society of america* 44, pp. 892–899.
- 682 Velikou, K., G. Lazoglou, K. Tolika, and C. Anagnostopoulou (2022). Reliability of the ERA5 in Replicat-
683 ing Mean and Extreme Temperatures across Europe. *Water* 14.4, p. 543. DOI: 10.3390/w14040543.
- 684 Venturas, M. D., H. N. Todd, A. T. Trugman, and W. R. L. Anderegg (2021). Understanding and
685 predicting forest mortality in the western United States using long-term forest inventory data and
686 modeled hydraulic damage. *New Phytologist* 230.5, pp. 1896–1910. DOI: 10.1111/nph.17043.
- 687 Vesk, P. A., W. K. Morris, W. C. Neal, K. Mokany, and L. J. Pollock (2021). Transferability of trait-based
688 species distribution models. *Ecography* 44.1, pp. 134–147. DOI: 10.1111/ecog.05179.
- 689 Zanne, A. E., W. D. Pearse, W. K. Cornwell, D. J. McGinn, I. J. Wright, et al. (2018). Functional
690 biogeography of angiosperms: life at the extremes. *New Phytologist* 218.4, pp. 1697–1709. DOI: 10.
691 1111/nph.15114.

1 Supporting Information for "Living on the edge - physiological
2 tolerance to frost and drought explains range limits of 35
3 European tree species"

4

5 **Contents**

6	1 Species list and details	2
7	1.1 Traits list -Trait values and references for LT_{50}	2
8	1.2 Supplementary references for LT_{50} measures	4
9	1.3 LT_{50} data filtering and additional measures	5
10	1.4 Traits list -Trait values and references for Ψ_{50}	7
11	1.5 Supplementary references for Ψ_{50} and Ψ_{88} measures	9
12	1.6 Additional measures of Ψ_{50}	13
13	2 Indicators of frost	14
14	3 Pedotransfer functions choice	15
15	4 Minimum soil potential scaling to the root system	17
16	4.1 Computing Gardener-Cowan coefficient, B_{GC}	17
17	4.2 Sensitivity of Ψ_{min} to SUREAU-ECOS parameters	18
18	5 Margin selection per species	22
19	6 Model selection per species	25
20	7 Generic model and transferability	29
21	8 Supplementary result figures	30
22	8.1 Correlation between percentiles of climatic variables and maximum experienced stress	30
23	8.2 Correlation between maximum experienced stress and frost and drought tolerance traits	32
24	8.3 Competitive dominance effect on the link between probability of presencee and safety margin?	33

25 1 Species list and details

26 The list of species studied~~and~~, associated measurements of Ψ_{50} , Ψ_{88} , and LT_{50} and associated references
 27 are shown in Tables S1 and S2.

28 1.1 ~~Traits-list~~ Trait values and references for LT_{50}

Species	LT_{50}	Reference
Abies alba	-41.13	Kreyling et al. 2015 Measured
Acer campestre	-33.13	Hofmann PhD 2015 Measured
Acer monspessulanum	-32.33	Hofmann PhD 2015 Measured
Acer platanoides	-38.79	Hofmann PhD 2015 Hofmann et al. 2014 Kreyling et al. 2015 Measured
Acer pseudoplatanus	-34.70	Charrier et al. 2013 Hofmann PhD 2015 Measured
Alnus glutinosa	-22.55	Hofmann PhD 2015 Hofmann et al. 2014
Alnus incana	-41.89	Measured
Arbutus unedo	-20.59	Hofmann PhD 2015 Measured
Betula pendula	-41.37	Charrier et al. 2013 Hofmann PhD 2015 Hofmann et al. 2014 Measured
Betula pubescens	-66.57	Measured
Carpinus betulus	-26.86	Charrier et al. 2013 Hofmann PhD 2015 Vitra et al. 2017
Corylus avellana	-24.45	Charrier et al. 2013
Fagus sylvatica	-33.23	Baffoin et al. 2021 Charra-Vaskou et al. 2012 Charrier et al. 2013 Hofmann PhD 2015 Hofmann et al. 2014 Kreyling et al. 2015 Kreyling et al. 2012 Lenz et al. 2016 Measured Vitra et al. 2017
Fraxinus excelsior	-23.90	Charrier et al. 2013 Hofmann PhD 2015
Ilex aquifolium	-25.02	Hofmann PhD 2015 Measured

Species	LT_{50}	Reference
<i>Juniperus communis</i>	-80.14	Measured
<i>Juniperus thurifera</i>	-22.33	Measured
<i>Larix decidua</i>	-35.83	Baffoin et al. 2021 Charra-Vaskou et al. 2012
<i>Olea europaea</i>	-7.76	Arias et al. 2017 Azarello et al. 2008 Barranco et al. 2005
<i>Picea abies</i>	-35.92	Charra-Vaskou et al. 2012 Hofmann PhD 2015 Hofmann et al. 2014 Kreyling et al. 2012 Measured
<i>Pinus nigra</i>	-43.92	Hofmann PhD 2015 Kreyling et al. 2015 Kreyling et al. 2012 Measured
<i>Pinus pinaster</i>	-21.36	Measured
<i>Pinus pinea</i>	-21.10	Measured
<i>Pinus sylvestris</i>	-50.31	Baffoin et al. 2021 Charrier et al. 2013 Hofmann PhD 2015 Kreyling et al. 2012 Li et al. 2020 Peguero-Pina et al. 2008 Repo et al. 1996
<i>Populus alba</i>	-31.00	Li et al. 2020 Sakai et al. 1981
<i>Populus nigra</i>	-22.33	Charrier et al. 2013 Sakai et al. 1981
<i>Prunus avium</i>	-26.57	Baffoin et al. 2021 Charrier et al. 2013 Hofmann PhD 2015 Vitra et al. 2017
<i>Prunus padus</i>	-32.97	Hofmann PhD 2015 Measured
<i>Quercus ilex</i>	-27.80	Hofmann PhD 2015 Morin et al. 2007
<i>Quercus petraea</i>	-35.82	Baffoin et al. 2021 Kreyling et al. 2015 Kreyling et al. 2012 Vitra et al. 2017
<i>Quercus pubescens</i>	-45.40	Kreyling et al. 2015 Morin et al. 2007
<i>Quercus robur</i>	-38.22	Baffoin et al. 2021 Charrier et al. 2013 Hofmann PhD 2015 Morin et al. 2007
<i>Quercus suber</i>	-24.26	Measured
<i>Sorbus aria</i>	-35.80	Hofmann PhD 2015 Measured
<i>Sorbus torminalis</i>	-31.76	Hofmann PhD 2015
<i>Taxus baccata</i>	-26.66	Hofmann PhD 2015

Species	LT_{50}	Reference
		Measured
Tilia cordata	-47.69	Hofmann PhD 2015 Hofmann et al. 2014
		Measured
Tilia platyphyllos	-35.89	Hofmann PhD 2015 Measured

Table 1: Species list, corresponding LT_{50} and reference. "Measured" refers to species for which we performed additional measures. The trait values correspond to the mean of measured LT_{50} and values in the references. See corresponding reference list in section S1.2

29 1.2 Supplementary references for LT_{50} measures

- 30 • Arias, N. S., Scholz, F. G., Goldstein, G., & Bucci, S. J. (2017). The cost of avoiding freezing in
31 stems: trade-off between xylem resistance to cavitation and supercooling capacity in woody plants.
32 Tree physiology, 37(9), 1251-1262.
- 33 • Azzarello, E., Mugnai, S., Pandolfi, C., Masi, E., Marone, E., & Mancuso, S. (2009). Comparing
34 image (fractal analysis) and electrochemical (impedance spectroscopy and electrolyte leakage)
35 techniques for the assessment of the freezing tolerance in olive. Trees, 23, 159-167.
- 36 • Baffoin, R., Charrier, G., Bouchardon, A. E., Bonhomme, M., Améglio, T., & Lacointe, A. (2021).
37 Seasonal changes in carbohydrates and water content predict dynamics of frost hardiness in various
38 temperate tree species. Tree Physiology, 41(9), 1583-1600.
- 39 • Barranco, D., Ruiz, N., & Gómez-del Campo, M. (2005). Frost tolerance of eight olive cultivars.
40 HortScience, 40(3), 558-560.
- 41 • Charra-Vaskou, K., Charrier, G., Wortemann, R., Beikircher, B., Cochard, H., Ameglio, T., &
42 Mayr, S. (2012). Drought and frost resistance of trees: a comparison of four species at different
43 sites and altitudes. Annals of Forest Science, 69(3), 325-333.
- 44 • Charrier, G., Poirier, M., Bonhomme, M., Lacointe, A., & Améglio, T. (2013). Frost hardiness in
45 walnut trees (*Juglans regia* L.): how to link physiology and modelling?. Tree Physiology, 33(11),
46 1229-1241.
- 47 • Hofmann PhD 2015
- 48 • Hofmann, M., Jager, M., & Bruelheide, H. (2014). Relationship between frost hardiness of adults
49 and seedlings of different tree species. iForest-Biogeosciences and Forestry, 7(5), 282.
- 50 • Kreyling, J., Schmid, S., & Aas, G. (2015). Cold tolerance of tree species is related to the climate
51 of their native ranges. Journal of Biogeography, 42(1), 156-166.
- 52 • Kreyling, J., Wiesenbergs, G. L., Thiel, D., Wohlfart, C., Huber, G., Walter, J., ... & Beierkuhnlein,
53 C. (2012). Cold hardiness of *Pinus nigra* Arnold as influenced by geographic origin, warming, and
54 extreme summer drought. Environmental and Experimental Botany, 78, 99-108.
- 55 • Lenz, A., Hoch, G., & Vitasse, Y. (2016). Fast acclimation of freezing resistance suggests no
56 influence of winter minimum temperature on the range limit of European beech. Tree Physiology,
57 36(4), 490-501.

- 58 • Li, S., Wu, F., Duan, Y., Singerman, A., & Guan, Z. (2020). Citrus greening: Management
59 strategies and their economic impact. *HortScience*, 55(5), 604-612.
- 60 • Morin, X., Améglio, T., Ahas, R., Kurz-Besson, C., Lanta, V., Lebourgeois, F., ... & Chuine, I.
61 (2007). Variation in cold hardiness and carbohydrate concentration from dormancy induction to
62 bud burst among provenances of three European oak species. *Tree physiology*, 27(6), 817-825.
- 63 • Peguero-Pina, J. J., Morales, F., & Gil-Pelegón, E. (2008). Frost damage in *Pinus sylvestris* L.
64 stems assessed by chlorophyll fluorescence in cortical bark chlorenchyma. *Annals of Forest Science*,
65 65(8), 1.
- 66 • Repo, T., Hänninen, H., & Kellomäki, S. (1996). The effects of long-term elevation of air tempera-
67 ture and CO on the frost hardiness of Scots pine. *Plant, Cell & Environment*, 19(2), 209-216.
- 68 • Sakai, A., Paton, D. M., & Wardle, P. (1981). Freezing resistance of trees of the south temperate
69 zone, especially subalpine species of Australasia. *Ecology*, 62(3), 563-570.
- 70 • Sutinen, M. L., Palta, J. P., & Reich, P. B. (1992). Seasonal differences in freezing stress resistance
71 of needles of *Pinus nigra* and *Pinus resinosa*: evaluation of the electrolyte leakage method. *Tree
72 Physiology*, 11(3), 241-254.
- 73 • Vitra, A., Lenz, A., & Vitasse, Y. (2017). Frost hardening and dehardening potential in temperate
74 trees from winter to budburst. *New Phytologist*, 216(1), 113-123.

75 1.3 LT_{50} data filtering and additional measures

76 We selected measurements performed in winter, because frost tolerance reaches a maximum in winter for
77 all species (Charrier et al., 2013), allowing to control for seasonal variation in LT_{50} . The LT_{50} estimates
78 varied with the methods of measure, the tree development stage and the organ. Accordingly, we selected
79 measures (i) performed using the electrolyte leakage or visual scoring method, which gives close and
80 accurate estimates (Lenz et al., 2013; Vitra et al., 2017), (ii) on adult trees (Charra-Vaskou et al., 2012),
81 and (iii) on branches or buds (these two organs did not display significant differences, p-value of the organ
82 class factor in anova of LT_{50} explained by species and organ: 0.1432).

83
84 We performed additional measures for 23 species of interest that were absent from our database or had
85 poor quality data: *Abies alba*, *Acer campestre*, *Acer platanoides*, *Acer monspessulanum*, *Acer pseudopla-
86 tanus*, *Alnus incana*, *Arbutus unedo*, *Betula pendula*, *Betulas pubescens*, *Fagus sylvatica*, *Ilex aquifolium*,
87 *Juniperus thurifera*, *Juniperus communis*, *Picea abies*, *Pinus nigra*, *Pinus pinaster*, *Pinus pinea*, *Prunus
88 padus*, *Quercus suber*, *Sorbus aria*, *Taxus baccata* *Tilia cordata*, *Tilia platyphyllos*. They were sampled
89 at the *Col des 3 Soeurs arboretum*, France (44.723543, 3.564722, 1500masl) and at the *Royat arboretum*,

90 France (45.755801, 3.024163, 800masl). We selected branches with multiple terminal twigs in five individual trees per species. We used the electrolyte leakage method to estimate LT_{50} .

92

93 For each individual, twigs were placed in a programmed freezer (Ministat Huber, Offenburg, Germany)
94 with an external Pt100 probe in the chamber. Freezing was applied at a steady rate of $5K.h^{-1}$ down
95 to -15, -25, -35 and -45°C. After 1 hour at the target temperature, samples were thawed to +5°C at a
96 constant rate of $5K.h^{-1}$. An additional sample was placed in a -80°C freezer and a control kept at 5°C.
97 After freezing treatments, the samples were cut into small sections and placed at +5°C on a rocking tube
98 shaker overnight in 15mL of ultrapure water. Then the quantity of damaged tissue in each sample is
99 estimated by measuring the electric conductivity of the solution (conductivity C1). Electrolytes are also
100 measured after destroying living tissue by placing the tubes in a standard lab autoclave (C2). Relative
101 electrolyte leakage (REL, %) at each temperature treatment is calculated as $REL = \frac{C_1}{C_2} \cdot 100$. We then fit
102 a four-parameter logistic function to the resulting response curves of REL to temperature in R. One model
103 was fit by species with individuals included as a random effect. LT_{50} was determined as the temperature
104 value at the inflection point of the sigmoid function :

$$y = \left[\frac{A}{(1 + e^{(B \cdot (C - x))})} \right] + D$$

105 Where y is the relative electrolyte leakage, x is the exposure temperature, parameters A and D define
106 the asymptotes of the function and B is the slope at the inflection point C.

¹⁰⁷ 1.4 ~~Traits list~~ Trait values and references for Ψ_{50}

Species	Ψ_{50}	Ψ_{88}	Reference
<i>Abies alba</i>	-3.85	-4.11	Bouche et al. 2014 Cochard 2006
<i>Acer campestre</i>	-5.10	-5.66	Li et al. 2016b Schumann et al. 2019 Measured
<i>Acer monspessulanum</i>	-6.74	-7.75	Martin St-Paul et al. 2017
<i>Acer platanoides</i>	-4.23	-5.25	Schumann et al. 2019
<i>Acer pseudoplatanus</i>	-3.28	-4.07	Li et al. 2016b Lubbe et al. 2017 Schumann et al. 2019
<i>Alnus glutinosa</i>	-1.49	-1.61	Hacke & Sauter 1996 Li et al. 2016a Zhang et al. 2018
<i>Alnus incana</i>	-1.45	-1.45	Hacke et al. 2001 Li et al. 2016a Sperry et al. 1994
<i>Betula pendula</i>	-1.81	-1.98	Brodribb et al. 2017 Cochard et al. 2005 Dulamsuren et al. 2019 Gonzalez-Munoz et al. 2018 Klepsch et al. 2016 Li et al. 2016a Zhang et al. 2018
<i>Betula pubescens</i>	-1.76	-1.98	Li et al. 2016a
<i>Carpinus betulus</i>	-4.17	-5.02	Dietrich et al. 2018 Li et al. 2016a Li et al. 2016b Lubbe et al. 2017 Tixier et al. 2014 Zhang et al. 2018
<i>Corylus avellana</i>	-2.03	-2.64	Kiorapostolou et al. 2019 Li & Jansen 2017 Li et al. 2016a Li et al. 2016b Zhang et al. 2018
<i>Fagus sylvatica</i>	-3.14	-4.06	Bar et al. 2018 Barigah et al. 2013 Charra-Vaskou et al. 2012 Cochard et al. 2005 Dietrich et al. 2018 Dusotoit-Coucaud et al. 2014 Hajek et al. 2016 Lubbe et al. 2017 Pivovaroff et al. 2016 Schuldt et al. 2016 Stojnic et al. 2018 Tixier et al. 2014 Tomasella et al. 2018

Species	Ψ_{50}	Ψ_{88}	Reference
			Urli et al. 2013
			Zhang et al. 2018
<i>Fraxinus excelsior</i>	-2.43	-4.38	Li et al. 2016b De Baerdemaeker et al. 2019a
			Zhang et al. 2018
<i>Ilex aquifolium</i>	-4.80		Li et al. 2016a
<i>Juniperus communis</i>	-6.37	-8.37	Beikircher & Mayr 2008 Cochard 2006 Mayr et al. 2006
<i>Juniperus thurifera</i>	-9.27	-12.16	Olano et al. 2017
<i>Larix decidua</i>	-3.47	-4.41	Bouche et al. 2014 Charra-Vaskou et al. 2012 Cochard 2006 Dietrich et al. 2018 Jansen et al. 2012 Mayr et al. 2006
<i>Olea europaea</i>	-5.30	-6.28	Quero et al. 2011 Torres-Ruiz et al. 2017a
<i>Picea abies</i>	-3.67	-4.54	Bar et al. 2018 Bouche et al. 2014 Charra-Vaskou et al. 2012 Cochard 2006 Cochard et al. 2005 Dietrich et al. 2018 Gonzalez-Munoz et al. 2018 Losso et al. 2017 Lu et al. 1996 Prendin et al. 2018 Tomasella et al. 2018
<i>Pinus nigra</i>	-3.52	-4.79	Jansen et al. 2012 Martinez-Vilalta & Pinol 2002 Measured
<i>Pinus pinaster</i>	-3.73	-4.29	Bouche et al. 2014 Bouche et al. 2016 Cochard 2006 Gauthney et al. 2020 Jansen et al. 2012 Lamy et al. 2014 Martinez-Vilalta & Pinol 2002 Pivovaroff et al. 2016 Zhang et al. 2018
<i>Pinus pinea</i>	-4.34	-4.90	Cochard 2006
<i>Pinus sylvestris</i>	-3.19	-4.35	Aguadz et al. 2015 Bar et al. 2018 Bouche et al. 2016 Cochard 2006 Cochard et al. 2005 Dietrich et al. 2018 Dulamsuren et al. 2019 Fang et al. 2018 Gonzalez-Munoz et al. 2018 Jin et al. 2018 Li et al. 2020a

Species	Ψ_{50}	Ψ_{88}	Reference
			Martinez-Vilalta & Pinol 2002
			Martinez-Vilalta et al. 2009
			Poyatos et al. 2007
			Torres-Ruiz et al. 2016
			Zhang et al. 2018
Populus alba	-1.52	-2.30	Hukin et al. 2005
Populus nigra	-2.02	-2.46	De Baerdemaeker et al. 2017 Guet et al. 2015
			Pivovaroff et al. 2016
Prunus avium	-4.77	-5.65	Cochard et al. 2007 Cochard et al. 2008
Prunus padus	-3.54	-4.01	Cochard et al. 2007 Cochard et al. 2008
Quercus ilex	-7.13	-9.33	Lobo et al. 2018
Quercus petraea	-4.60	-5.75	Dietrich et al. 2018 Lobo et al. 2018
			Torres-Ruiz et al. 2019
Quercus pubescens	-5.10	-5.40	Martin St-Paul et al. 2017
Quercus robur	-4.74	-5.66	Lobo et al. 2018
Quercus suber	-5.52	-7.93	Lobo et al. 2018
Sorbus aria	-5.67		Tixier et al. 2014
Taxus baccata	-6.73	-9.05	Bouche et al. 2014 Cochard 2006
Tilia cordata	-3.22	-3.94	Kiorapostolou et al. 2019 Lubbe et al. 2017

Table 2: Species list, corresponding Ψ_{50} , Ψ_{88} and reference. "Measured" refers to species for which we performed additional measures. The trait values correspond to the mean of measured Ψ_{50} and values in the references. See corresponding reference list in section S1.5

108 1.5 Supplementary references for Ψ_{50} and Ψ_{88} measures

- 109 • Bär, A., Nardini, A., & Mayr, S. (2018). Post-fire effects in xylem hydraulics of *Picea abies*, *Pinus*
110 *sylvestris* and *Fagus sylvatica*. *The New Phytologist*, 217(4), 1484–1493. doi:10.1111/nph.14916
- 111 • Barigah, T. S., Charrier, O., Douris, M., Bonhomme, M., Herbette, S., Améglio, T., ... Cochard,
112 H. (2013). Water stress-induced xylem hydraulic failure is a causal factor of tree mortality in beech
113 and poplar. *Annals of Botany*, 112(7), 1431–1437. doi:10.1093/aob/mct204
- 114 • Beikircher, B., & Mayr, S. (2008). The hydraulic architecture of *Juniperus communis* L. ssp. *communis*: shrubs and trees compared. *Plant, Cell & Environment*, 31(11), 1545–1556. doi:10.1111/j.1365-
115 3040.2008.01860.x
- 116 • Bouche, P. S., Jansen, S., Sabalera, J. C., Cochard, H., Burlett, R., & Delzon, S. (2016). Low
117 intra-tree variability in resistance to embolism in four Pinaceae species. *Annals of Forest Science*,
118 73(3), 681–689. doi:10.1007/s13595-016-0553-6
- 119 • Bouche, P. S., Larter, M., Domec, J.-C., Burlett, R., Gasson, P., Jansen, S., & Delzon, S. (2014). A
120 broad survey of hydraulic and mechanical safety in the xylem of conifers. *Journal of Experimental
121 Botany*, 65(15), 4419–4431. doi:10.1093/jxb/eru218

- 123 • Brodribb, T. J., Carriqui, M., Delzon, S., & Lucani, C. (2017). Optical measurement of stem xylem
124 vulnerability. *Plant Physiology*, 174(4), 2054–2061.
125 doi:10.1104/pp.17.00552
- 126 • Charra-Vaskou, K., Charrier, G., Wortemann, R., Beikircher, B., Cochard, H., Ameglio, T., &
127 Mayr, S. (2012). Drought and frost resistance of trees: a comparison of four species at different
128 sites and altitudes. *Annals of Forest Science*, 69(3), 325–333. doi:10.1007/s13595-011-0160-5
- 129 • Cochard, H., Peiffer, M., Le Gall, K., & Andre, G. (1997). Developmental control of xylem hydraulic
130 resistances and vulnerability to embolism in *Fraxinus excelsior* L.: impacts on water relations.
131 *Journal of Experimental Botany*, 48(3), 655–663. doi:10.1093/jxb/48.3.655
- 132 • Cochard, Hervé, Barigah, S. T., Kleinhentz, M., & Eshel, A. (2008). Is xylem cavitation resis-
133 tance a relevant criterion for screening drought resistance among *Prunus* species? *Journal of Plant
134 Physiology*, 165(9), 976–982. doi:10.1016/j.jplph.2007.07.020
- 135 • Cochard, Hervé, Casella, E., & Mencuccini, M. (2007). Xylem vulnerability to cavitation varies
136 among poplar and willow clones and correlates with yield. *Tree Physiology*, 27(12), 1761–1767.
137 doi:10.1093/treephys/27.12.1761
- 138 • Cochard, Hervé, Damour, G., Bodet, C., Tharwat, I., Poirier, M., & Améglio, T. (2005). Evalu-
139 ation of a new centrifuge technique for rapid generation of xylem vulnerability curves. *Physiologia
140 Plantarum*, 124(4), 410–418. doi:10.1111/j.1399-3054.2005.00526.x
- 141 • Cochard, Hervé. (2006). Cavitation in trees. *Comptes Rendus. Physique*, 7(9–10), 1018–1026.
142 doi:10.1016/j.crhy.2006.10.012
- 143 • De Baerdemaeker, N. J. F., Salomón, R. L., De Roo, L., & Steppe, K. (2017). Sugars from
144 woody tissue photosynthesis reduce xylem vulnerability to cavitation. *The New Phytologist*, 216(3),
145 720–727. doi:10.1111/nph.14787
- 146 • De Baerdemaeker, N. J. F., Stock, M., Van den Bulcke, J., De Baets, B., Van Hoorebeke, L., &
147 Steppe, K. (2019). X-ray microtomography and linear discriminant analysis enable detection of
148 embolism-related acoustic emissions. *Plant Methods*, 15(1), 153. doi:10.1186/s13007-019-0543-4
- 149 • Dietrich, L., Hoch, G., Kahmen, A., & Körner, C. (2018). Losing half the conductive area hardly
150 impacts the water status of mature trees. *Scientific Reports*, 8(1), 15006. doi:10.1038/s41598-018-
151 33465-0
- 152 • Dulamsuren, C., Abilova, S. B., Bektayeva, M., Eldarov, M., Schultdt, B., Leuschner, C., & Hauck,
153 M. (2019). Hydraulic architecture and vulnerability to drought-induced embolism in southern boreal
154 tree species of Inner Asia. *Tree Physiology*, 39(3), 463–473. doi:10.1093/treephys/tpy116
- 155 • Dusotoit-Coucaud, A., Brunel, N., Tixier, A., Cochard, H., & Herbette, S. (2014). Hydrolase
156 treatments help unravel the function of intervessel pits in xylem hydraulics. *Physiologia Plantarum*,
157 150(3), 388–396. doi:10.1111/ppl.12092
- 158 • Gauthey, A., Peters, J. M. R., Carins-Murphy, M. R., Rodriguez-Dominguez, C. M., Li, X., Delzon,
159 S., ... Choat, B. (2020). Visual and hydraulic techniques produce similar estimates of cavitation
160 resistance in woody species. *The New Phytologist*, 228(3), 884–897. doi:10.1111/nph.16746
- 161 • González-Muñoz, N., Sterck, F., Torres-Ruiz, J. M., Petit, G., Cochard, H., von Arx, G., ... Delzon,
162 S. (2018). Quantifying in situ phenotypic variability in the hydraulic properties of four tree species
163 across their distribution range in Europe. *PloS One*, 13(5), e0196075. doi:10.1371/journal.pone.0196075

- 164 • Guet, J., Fichot, R., Lédée, C., Laurans, F., Cochard, H., Delzon, S., ... Brignolas, F. (2015).
165 Stem xylem resistance to cavitation is related to xylem structure but not to growth and water-
166 use efficiency at the within-population level in *Populus nigra* L. *Journal of Experimental Botany*,
167 66(15), 4643–4652. doi:10.1093/jxb/erv232
- 168 • Hacke, U. G., Sperry, J. S., Pockman, W. T., Davis, S. D., & McCulloh, K. A. (2001). Trends
169 in wood density and structure are linked to prevention of xylem implosion by negative pressure.
170 *Oecologia*, 126(4), 457–461. doi:10.1007/s004420100628
- 171 • Hacke, U., & Sauter, J. J. (1996). Drought-Induced Xylem Dysfunction in Petioles, Branches,
172 and Roots of *Populus balsamifera* L. and *Alnus glutinosa* (L.) Gaertn. *Plant Physiology*, 111(2),
173 413–417. doi:10.1104/pp.111.2.413
- 174 • Hammond, W., Choat, B., Johnson, D., Ali Ahmed, M., Anderegg, L., Barigah, T. S., Barros, F.,
175 Bartlett, M., Bauerle, T., Beikircher, B., Bittencourt, P., Blackman, C., Brodribb, T., Brum, M.,
176 Cano, J., Cardoso, A., Chen, Y., Carmesin, C., Cochard, H., ... Jansen, S. (2021). The global
177 vulnerability of plant xylem. AGUFM, 2021, B31F-07.
178 <https://ui.adsabs.harvard.edu/abs/2021AGUFM.B31F..07H/abstract>
- 179 • Hukin, D., Cochard, H., Dreyer, E., Le Thiec, D., & Bogeat-Triboulot, M. B. (2005). Cavitation
180 vulnerability in roots and shoots: does *Populus euphratica* Oliv., a poplar from arid areas of
181 Central Asia, differ from other poplar species? *Journal of Experimental Botany*, 56(418), 2003–2010.
182 doi:10.1093/jxb/eri198
- 183 • Jansen, S., Lamy, J.-B., Burlett, R., Cochard, H., Gasson, P., & Delzon, S. (2012). Plasmodesmal
184 pores in the torus of bordered pit membranes affect cavitation resistance of conifer xylem. *Plant,*
185 *Cell & Environment*, 35(6), 1109–1120. doi:10.1111/j.1365-3040.2011.02476.x
- 186 • Kiorapostolou, N., Da Sois, L., Petrizzellis, F., Savi, T., Trifilò, P., Nardini, A., & Petit, G. (2019).
187 Vulnerability to xylem embolism correlates to wood parenchyma fraction in angiosperms but not
188 in gymnosperms. *Tree Physiology*, 39(10), 1675–1684. doi:10.1093/treephys/tpz068
- 189 • Klepsch, M., Zhang, Y., Kotowska, M. M., Lamarque, L. J., Nolf, M., Schuldt, B., ... Jansen,
190 S. (2018). Is xylem of angiosperm leaves less resistant to embolism than branches? Insights
191 from microCT, hydraulics, and anatomy. *Journal of Experimental Botany*, 69(22), 5611–5623.
192 doi:10.1093/jxb/ery321
- 193 • Lamy, J.-B., Delzon, S., Bouche, P. S., Alia, R., Vendramin, G. G., Cochard, H., & Plomion, C.
194 (2014). Limited genetic variability and phenotypic plasticity detected for cavitation resistance in a
195 Mediterranean pine. *The New Phytologist*, 201(3), 874–886. doi:10.1111/nph.12556
- 196 • Li, S., & Jansen, S. (2017). The root cambium ultrastructure during drought stress in *Corylus*
197 *avellana*. *IAWA Journal*, 38(1), 67–80. doi:10.1163/22941932-20170157
- 198 • Li, S., Feifel, M., Karimi, Z., Schuldt, B., Choat, B., & Jansen, S. (2016). Leaf gas exchange per-
199 formance and the lethal water potential of five European species during drought. *Tree Physiology*,
200 36(2), 179–192. doi:10.1093/treephys/tpv117
- 201 • Li, S., Lens, F., Espino, S., Karimi, Z., Klepsch, M., Schenk, H. J., ... Jansen, S. (2016). Intervessel
202 pit membrane thickness as a key determinant of embolism resistance in angiosperm xylem. *IAWA*
203 *Journal*, 37(2), 152–171. doi:10.1163/22941932-20160128
- 204 • Lobo, A., Torres-Ruiz, J. M., Burlett, R., Lemaire, C., Parise, C., Francioni, C., ... Delzon, S.
205 (2018). Assessing inter- and intraspecific variability of xylem vulnerability to embolism in oaks.
206 *Forest Ecology and Management*, 424, 53–61. doi:10.1016/j.foreco.2018.04.031

- 207 • Losso, A., Beikircher, B., Dämon, B., Kikuta, S., Schmid, P., & Mayr, S. (2017). Xylem sap surface
208 tension may be crucial for hydraulic safety. *Plant Physiology*, 175(3), 1135–1143. doi:10.1104/pp.17.01053
- 209 • Lu, P., Biron, P., Granier, A., & Cochard, H. (1996). Water relations of adult Norway spruce
210 (*Picea abies* (L.) Karst) under soil drought in the Vosges mountains: whole-tree hydraulic conduc-
211 tance, xylem embolism and water loss regulation. *Annales Des Sciences Forestières*, 53(1), 113–121.
212 doi:10.1051/forest:19960108
- 213 • Lübbe, T., Schultdt, B., & Leuschner, C. (2017). Acclimation of leaf water status and stem hydraulics
214 to drought and tree neighbourhood: alternative strategies among the saplings of five temperate
215 deciduous tree species. *Tree Physiology*, 37(4), 456–468. doi:10.1093/treephys/tpw095
- 216 • Martinez-Vilalta, J., & Pinol, J. (2002). Drought-induced mortality and hydraulic architecture in
217 pine populations of the NE Iberian Peninsula. *Forest Ecology and Management*, 161(1–3), 247–256.
218 doi:10.1016/s0378-1127(01)00495-9
- 219 • Martin-StPaul, N., Delzon, S., Cochard, H. (2017). Plant resistance to drought depends on timely
220 stomatal closure. *Ecology Letters*, 20(11), 1437–1447.
221 <https://doi.org/10.1111/ele.12851>
- 222 • Mayr, S., Hacke, U., Schmid, P., Schwienbacher, F., & Gruber, A. (2006). Frost drought in
223 conifers at the alpine timberline: xylem dysfunction and adaptations. *Ecology*, 87(12), 3175–3185.
224 doi:10.1890/0012-9658(2006)87[3175:fdicat]2.0.co;2
- 225 • Mayr, S., Rothart, B., & Dämon, B. (2003). Hydraulic efficiency and safety of leader shoots and
226 twigs in Norway spruce growing at the alpine timberline. *Journal of Experimental Botany*, 54(392),
227 2563–2568. doi:10.1093/jxb/erg272
- 228 • Mayr, S., Schwienbacher, F., & Bauer, H. (2003). Winter at the alpine timberline. Why does
229 embolism occur in norway spruce but not in stone pine? *Plant Physiology*, 131(2), 780–792.
230 doi:10.1104/pp.011452
- 231 • Mayr, S., Wolfschwenger, M., & Bauer, H. (2002). Winter-drought induced embolism in Norway
232 spruce (*Picea abies*) at the Alpine timberline. *Physiologia Plantarum*, 115(1), 74–80. doi:10.1034/j.1399-
233 3054.2002.1150108.x
- 234 • Pivovaroff, A. L., Burlett, R., Lavigne, B., Cochard, H., Santiago, L. S., & Delzon, S. (2016).
235 Testing the ‘microbubble effect’ using the Cavitron technique to measure xylem water extraction
236 curves. *AoB Plants*, 8, lw011. doi:10.1093/aobpla/plw011
- 237 • Prendin, A. L., Mayr, S., Beikircher, B., von Arx, G., & Petit, G. (2018). Xylem anatomical
238 adjustments prioritize hydraulic efficiency over safety as Norway spruce trees grow taller. *Tree
239 Physiology*, 38(8), 1088–1097. doi:10.1093/treephys/tpy065
- 240 • Quero, J. L., Sterck, F. J., Martínez-Vilalta, J., & Villar, R. (2011). Water-use strategies of six
241 co-existing Mediterranean woody species during a summer drought. *Oecologia*, 166(1), 45–57.
242 doi:10.1007/s00442-011-1922-3
- 243 • Rico, C., Pittermann, J., Polley, H. W., Aspinwall, M. J., & Fay, P. A. (2013). The effect of
244 subambient to elevated atmospheric CO₂ concentration on vascular function in *Helianthus annuus*:
245 implications for plant response to climate change. *The New Phytologist*, 199(4), 956–965.
246 doi:10.1111/nph.12339

- 247 • Schumann, K., Leuschner, C., & Schuldt, B. (2019). Xylem hydraulic safety and efficiency in
248 relation to leaf and wood traits in three temperate Acer species differing in habitat preferences.
249 *Trees* (Berlin, Germany: West), 33(5), 1475–1490. doi:10.1007/s00468-019-01874-x
- 250 • Sperry, J. S., Nichols, K. L., Sullivan, J. E. M., & Eastlack, S. E. (1994). Xylem embolism in
251 ring-porous, diffuse-porous, and coniferous trees of northern Utah and interior Alaska. *Ecology*,
252 75(6), 1736–1752. doi:10.2307/1939633
- 253 • Tixer, A., Herbette, S., Jansen, S., Capron, M., Tordjeman, P., Cochard, H., & Badel, E. (2014).
254 Modelling the mechanical behaviour of pit membranes in bordered pits with respect to cavitation
255 resistance in angiosperms. *Annals of Botany*, 114(2), 325–334. doi:10.1093/aob/mcu109
- 256 • Tomasella, M., Beikircher, B., Häberle, K.-H., Hesse, B., Kallenbach, C., Matyssek, R., & Mayr, S.
257 (2018). Acclimation of branch and leaf hydraulics in adult *Fagus sylvatica* and *Picea abies* in a forest
258 through-fall exclusion experiment. *Tree Physiology*, 38(2), 198–211. doi:10.1093/treephys/tpx140
- 259 • Torres-Ruiz, J. M., Kremer, A., Carins Murphy, M. R., Brodribb, T., Lamarque, L. J., Truffaut,
260 L., ... Delzon, S. (2019). Genetic differentiation in functional traits among European sessile oak
261 populations. *Tree Physiology*, 39(10), 1736–1749. doi:10.1093/treephys/tpz090
- 262 • Zhang, Y., Lamarque, L. J., Torres-Ruiz, J. M., Schuldt, B., Karimi, Z., Li, S., ... Jansen, S.
263 (2018). Testing the plant pneumatic method to estimate xylem embolism resistance in stems of
264 temperate trees. *Tree Physiology*, 38(7), 1016–1025. doi:10.1093/treephys/tpy015

265 1.6 Additional measures of Ψ_{50}

266 Additional measurements were performed using a Cavitron which allows accurate and rapid estimation
267 of embolism resistance (Cochard, 2006). Briefly, the Cavitron consists of a large rotor on which branch
268 samples are fixed with both extremities in a cuvette containing water. As the centrifuge spins, water flows
269 from one cuvette to the other through the sample, with flow related to the amount of embolism on the
270 xylem of the sample. As speed is increased, the pressure in the xylem becomes more negative, similarly
271 to what occurs in plants during drought. As embolism occurs, the percentage loss of conductivity (PLC)
272 is measured as a function of the pressure applied (Cochard, 2002; Pammenter and Van der Willigen,
273 1998), resulting in a sigmoid vulnerability curve (VC) from which the inflection point Ψ_{50} is determined,
274 which corresponds to the xylem pressure inducing a 50% loss of hydraulic conductance. For data from
275 the literature, to avoid using data suffering from the “open-vessel” artefact, we filtered out VCs that were
276 not a sigmoid shape. Ψ_{50} is deduced from PLC curves (see Delzon et al., 2010 for detailed methods).

277 2 Indicators of frost

278 All computations of T_{min} were done with the climatic data operator CDO (Schulzweida, 2022). The map
279 of T_{min} used is presented in figure S1. The various methods for estimating extreme values recommend
280 calibrating an extreme value model on a time series to extract the percentiles. However, at the European
281 scale, this method is complicated to apply, as it is very demanding in terms of computing power and
282 time. We therefore used the 5th percentile corresponding to an extreme temperature with a 20 years
283 return rate. To check the accuracy of this method, we selected randomly 100 points and compared the
284 values calculated with percentiles with those obtained with extreme value distribution (EVD) (as done
285 in Kollas et al., 2014). We found that the two estimates are closely related.

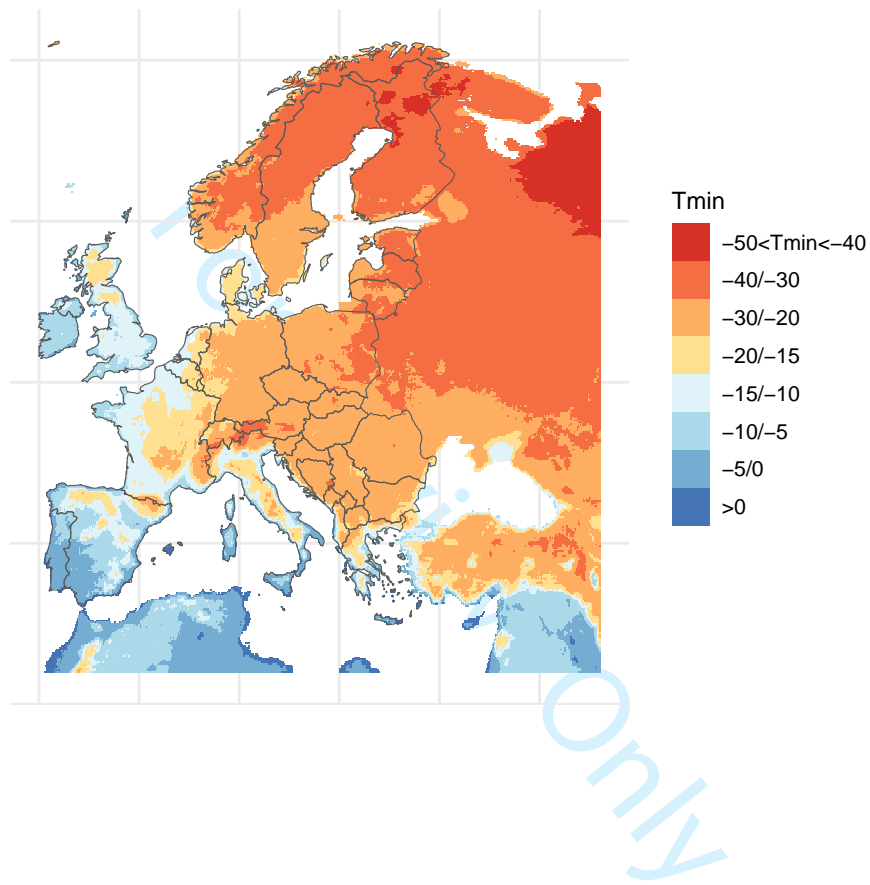


Figure 1: Map of T_{min} in °C.

286 3 Pedotransfer functions choice

287 There are different sets of pedotransfer equations (Sperry et al., 1998; Van Genuchten, 1980), each with
288 different sets of parameters depending on the geographical calibration zone. Pedotransfer functions are
289 very non-linear, and thus highly sensitive to variation in θ and soil texture parameters. Depending on
290 the method of θ_{min} computation, the resolution of the textures, the parameters of the formula and the

291 formula itself, the results can vary by several orders of magnitude. ERA5-land reanalysis uses the Van
292 Genuchten soil moisture retention curves for the computation of soil hydraulic transfer. For consistency,
293 we chose these equations. We used the parameters computed spatially over all Europe by Tóth et al.,
294 2017. They vary continuously with the different composition of soil texture (see Fig. S2).

295

296 Because the horizons of Tóth et al., 2017 did not match those of ERA-5 land data, we weighted each
297 ERA5-land horizons by their overlapping width with Toth's horizons, so we could build fictive horizons
298 from ERA5-land with an equivalent width than that of hydraulic parameters (see Table S3).

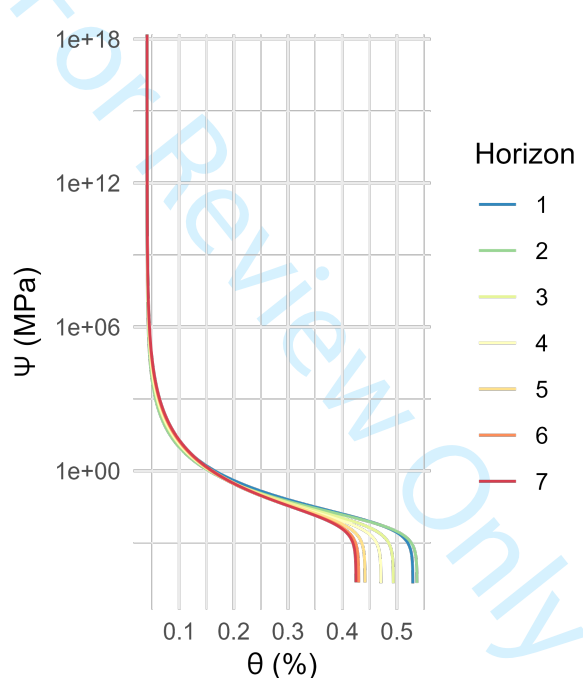


Figure 2: Van Genuchten models for the mean parameters of the seven horizons. The model gives the soil potential according to the soil water content θ and the soil horizon. The highest numbers are associated with the deepest horizons

Horizon depth (cm)	ERA5-land horizon	Toth horizon
5	1	1
7	1	2
15	2	2
28	2	3
30	3	3
60	3	4
100	3	5
200	4	6
280	4	7

Table 3: Matching between soil horizons of the (Tóth et al., 2017) dataset and horizons from ERA5-land.

299 4 Minimum soil potential scaling to the root system

300 4.1 Computing Gardner-Cowan coefficient, B_{GC}

301 Based on empirical equation (Martin-StPaul et al., 2017), B_{GC} was computed as follow for each h horizon

302 :

$$B_{GC,h} = \frac{2 \cdot \pi \cdot L_{a,h}}{\ln(\frac{b_h}{r})} \quad (1)$$

$$b_h = \frac{1}{\sqrt{\pi \cdot L_{v,h}}} \quad (2)$$

303 With r the fine root mean radius set to 0.0004m, $L_{a,h}$ the root length per unit area and the $L_{v,h}$ root
304 length per unit volume.

305 We assumed a root-to-leaf ratio of 1, thus meaning that the fine root area index was equal to the leaf
306 area index (LAI), set at $5m^2/m^2$. The sensitivity of Ψ_{min} to the LAI assumption is discussed hereafter.
307 Using the fine root proportion in each soil horizon, we computed the root length per unit area $L_{a,h}$ and
308 the root length per unit volume $L_{v,h}$ as follow:

$$L_{a,h} = \frac{LAI \cdot p_{root,h}}{2 \cdot \pi \cdot r} \quad (3)$$

$$L_{v,h} = \frac{L_{a,h}}{2 \cdot \pi \cdot r \cdot d_h} \quad (4)$$

(5)

With $p_{root,h}$ the proportion of roots in the horizon h , d_h its depth, r the fine root mean radius set to 0.0004m, LAI the Leaf Area Index set to $5m^2/m^2$.

The proportion of fine root in each soil layer $p_{root,h}$ was computed assuming a constant root area for all pixels and applying an average root profile decline with soil depth. As we did not have specific information on the root profiles of all the species in our study, we used the root profiles from Jackson et al., 1996 which provide estimates of root profiles per biomes at global scale. This is based on the following equation:

$$F_{root}(d) = 1 - \beta^d \quad (6)$$

Where $F_{root}(d)$ is the distribution function of roots at a soil depth d , in centimeters, and β is a numerical index of rooting distribution varying according to biomes. We set β to 0.97 as proposed in SUREAU-ECOS and corresponding to the average of the two most frequent biomes in Europe - coniferous and deciduous temperate forest. We discussed the sensitivity of Ψ_{min} to β hereafter. The proportion of roots per horizons $p_{root,h}$ was computed for each soil layer from the distribution function and scaled to the total root proportion of the profile $1 - \beta^{d_{max}}$, with d_{max} the maximum soil depth of each location extracted from (Hiederer, 2013) at 1 km resolution. We chose to account for variability in soil depth which is critical for our estimation of maximum drought stress. There is a large uncertainty inherent to soil depth maps, but this is the best estimate we can use and probably better than using a constant depth.

4.2 Sensitivity of Ψ_{min} to SUREAU-ECOS parameters

Sensitivity analysis methods

Root profile The study by Jackson et al., 1996 provides values for the parameter β for different biomes,

328 ranging from 0.943 to 0.976. We calculated Ψ_{min} with a β value that varies according to the biomes
 329 considered, using the WWF biome limits ([Olson2001](#)[Olson et al., 2001](#), see Table S4 for correspondence
 330 between Jackson et al., 1996 and WWF). In doing so, we assume that species' root profile have a plastic
 331 variation between biomes. The sensitivity analysis of Ψ_{min} computation to variations in β within this
 332 range gave 11% bias, and the correlation was as high as 0.99. Moreover, the log-RMSE was 1.49kPa. The
 333 figure S3 shows the differences between each computation method. It shows in particular that adding a
 334 variation in root profile per biome, slightly changes the values of Ψ_{min} observed in mountainous areas,
 335 about +/- 0.5 MPa. However, as the sensitivity of Ψ_{min} to β remains low overall and the determination
 336 of root profiles is subject to considerable uncertainties, we preferred to keep the root profile constant (*i.e.*
 337 constant β).

338

WWF biome	Jackson et al., 1996 biomes	β
Temperate Broadleaf and Mixed Forests	Temperate deciduous forest	0.966
Temperate Conifer Forests	15 Temperate coniferous forest	0.976
Mediterranean Forests, Woodlands and Scrub	Sclerophyllous shrubs	0.964
Boreal forest, taiga	Boreal forests	0.943
Tundra	Tundra	0.913

Table 4: Matching between WWF biomes and Jackson et al., 1996 biomes values

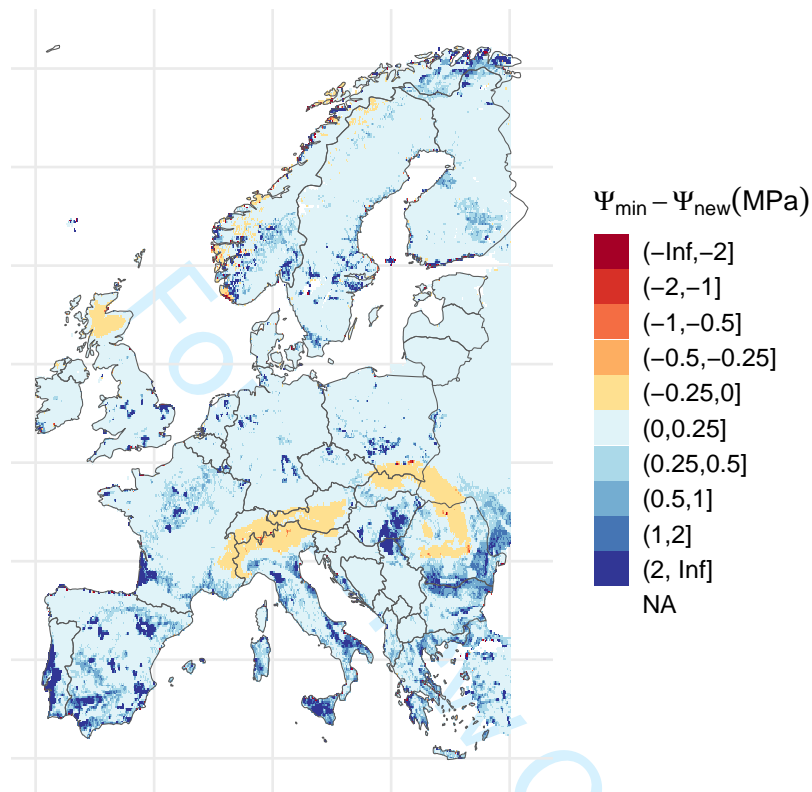


Figure 3: Map of differences in Ψ_{min} between computation with a constant with β (Ψ_{min}) and computation with β varying between biomes (Ψ_{new}).

339 *LAI* We tested the sensitivity of the minimum soil potential to LAI values and compared it to the
 340 reference of $5\text{ m}^2/\text{m}^2$. We chose values varying from 2 to $8\text{ m}^2/\text{m}^2$, in steps of $1\text{ m}^2/\text{m}^2$, following observed
 341 variability in Europe (Leuschner and Meier, 2018). We did not find any significant bias, lowest p-value
 342 was 0.992. The correlations were higher than 0.99 for the LAI values tested and the log-RMSE were
 343 1.00kPa for all LAI. This indicated that Ψ_{min} was not very sensitive to LAI variation (figure S4). And
 344 we kept a value of $5\text{ m}^2/\text{m}^2$ all over Europe, which is the value used in SUREAU-ECOS (Martin-StPaul
 345 et al., 2017).

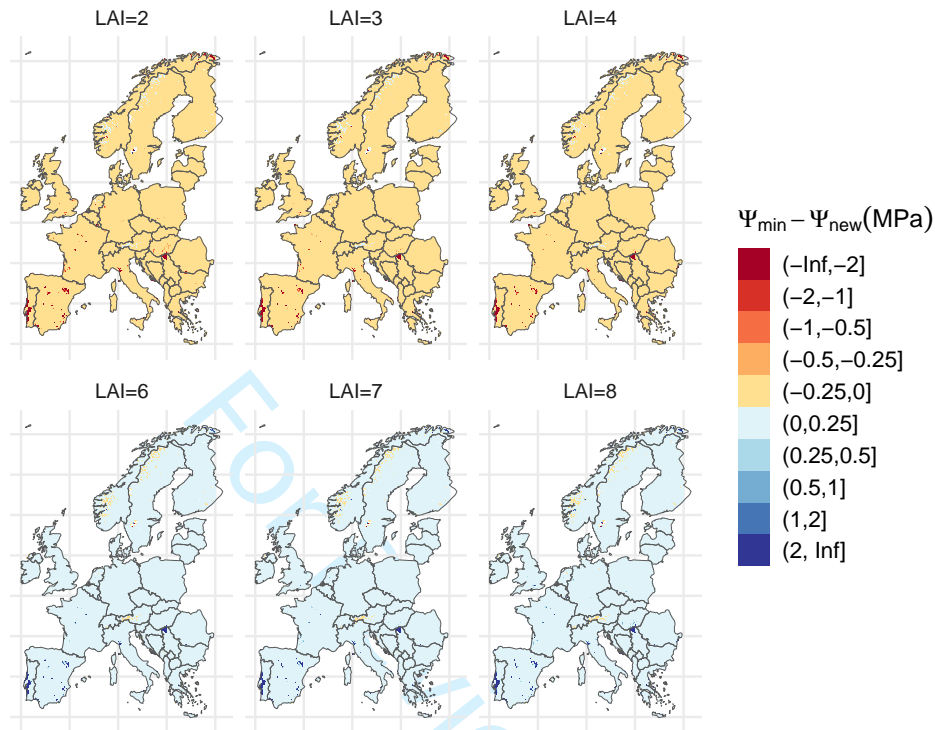


Figure 4: Map of differences in Ψ_{min} between reference computation with $LAI = 5\text{m}^2/\text{m}^2$ and computation with other values of LAI . Negative difference indicates that reference is lower than new computation.

346 Sensitivity analysis conclusion Ψ_{min} was the most sensitive to the root profile parameter β . Therefore,
 347 we fitted all models using a β varying between biomes, and run again the analysis. Inferred parameters
 348 and main conclusion remained almost unchanged (figure S5). The same model (FSM, HSM, or both) was
 349 selected for all species.

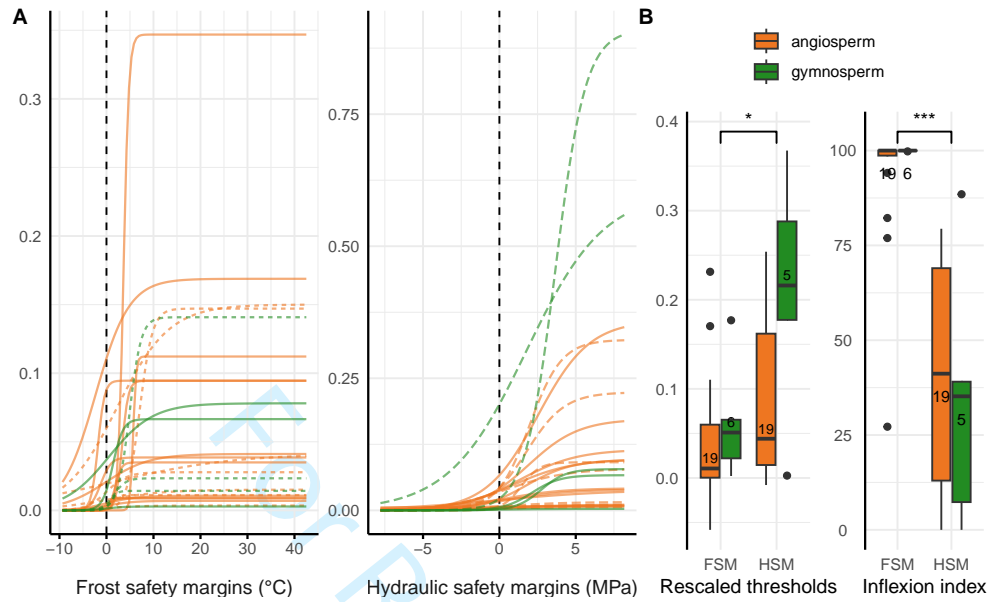


Figure 5: Predicted probability of presence as a function of *FSM* and *HSM* (A) and parameters of the function describing the shift in probability of presence - the rescaled threshold t and the inflexion index I . (B). Models were run using a β varying between biomes. A. Predictions are made from the mean model outputs and with the other safety margins fixed at its 95th percentiles. Colors highlight differences between angiosperms (orange) and gymnosperms (green). Dashed lines represent species with a model including only one safety margin. B. Metrics of the model: thresholds t rescaled by the range safety margin for the species, and the inflexion index I computed as the ratio between the slope r at the inflexion t and at 95th percentiles of the safety margin range. The number of species in each distribution is shown in the boxplots. Difference between groups, i.e. *HSM* vs. *FSM*, were tested with t-test, and indicated when significant with *, **, or ***, corresponding respectively to p-value less than 0.05, 0.01 and 0.001.

350 5 Margin selection per species

351 For each species, we checked whether occurrence data enabled to cover the distribution limit at its cold
 352 and dry margin. Figure S6 details how we perform this analysis and gives an example of a species for
 353 which the ~~dry-cold~~ margin is not well covered, but the ~~cold-dry~~ margin is. ~~Briefly, we compared For the~~
 354 ~~cold margin, we computed~~ the 5th percentiles of ~~mat -for the cold margin-~~ (95th percentiles of ~~pet -for the~~
 355 ~~dry margin)~~ calculated with all points falling either inside or outside over all the absences falling outside
 356 the distribution and over the occurrence (absence or presence) falling inside the expert-based EuForGen
 357 distribution. Note we took all the occurrences inside EuForGen for computing percentiles of the species
 358 distribution, to deal with species that would have very low prevalence and for which percentiles would
 359 not represent well the limit of the expert map. If the 5th percentile of ~~mat inside the distribution was~~
 360 ~~lower than absences was below the 5th percentile of mat outside the distribution inside occurrences, then~~

361 the distribution limit at the cold margin was ~~not~~ covered by the EuForest data~~(same approach for the~~.
362 The approach was the same with the dry margin, ~~if the using 95th percentile percentiles of pet~~inside the
363 ~~distribution is higher than outside, then the dry margin is not covered by the data).~~ The Table. The
364 ~~table~~ S6 summarises for each species whether the margin could be tested or not (column “Cold margin”
365 and “Dry margin”, TRUE/FALSE).

For Review Only

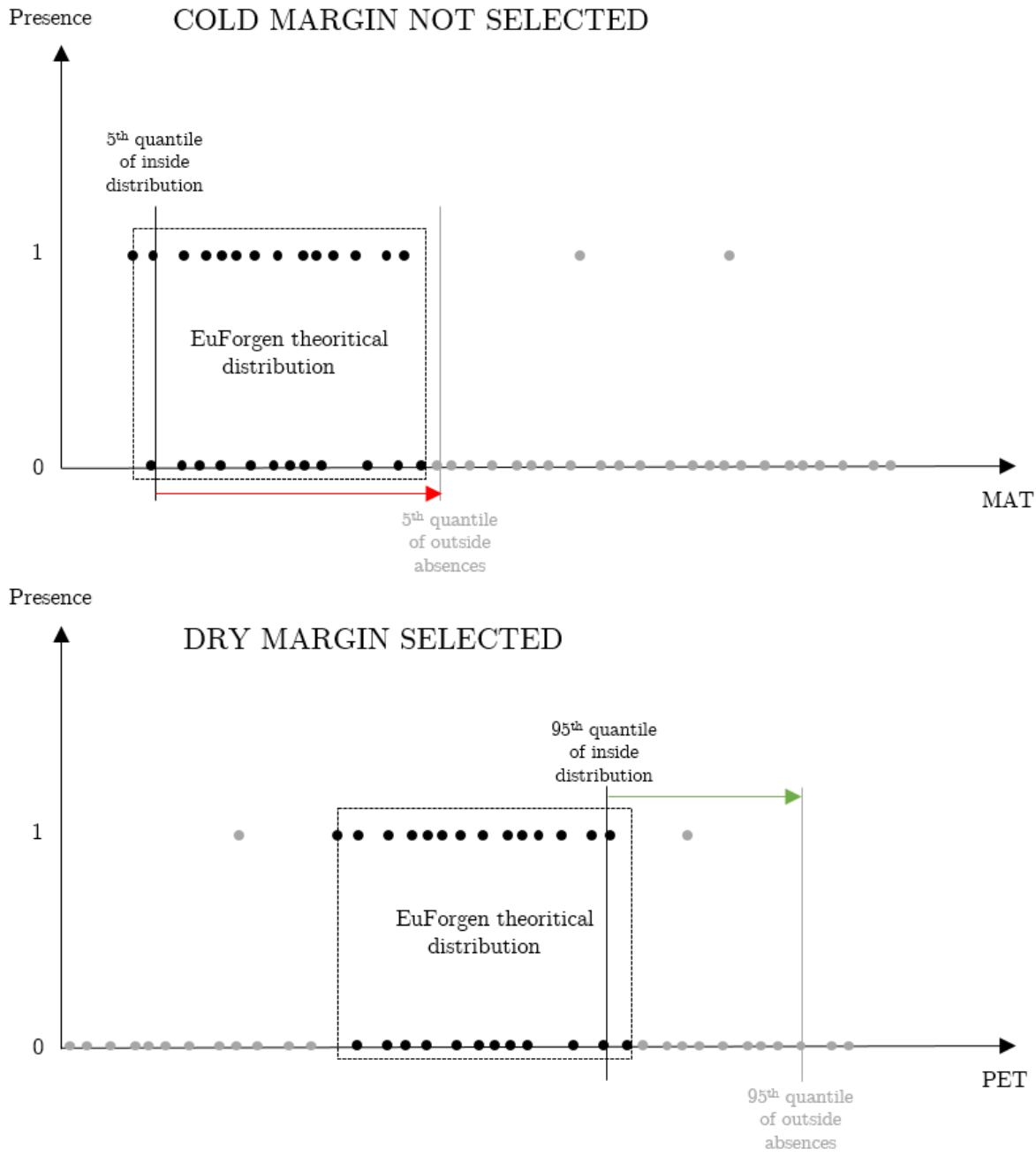


Figure 6: Method for determining whether presence/absence data capture the distribution limits in the cold and dry margins. In the upper panel, absences are not distributed in colder conditions than the EuForgen distribution. The cold margin limit is not captured by the data and the *FSM* cannot be used to explain the distribution. In the lower panel, absences are distributed beyond the dry margin of the EuForgen distribution, and *HSM* can be used to explain the distribution.

366 6 Model selection per species

367 For each species we fitted four models, with two, one or none safety margins. Models with margins not
 368 covered by the distribution of the species were excluded. The four possible models were the following :

HSM & FSM : (7)

$$p_{i,j} = \frac{K_j}{[1 + \exp(-r_{FSM,j} \cdot (FSM[i,j] - t_{FSM,j}))] \cdot [1 + \exp(-r_{HSM,j} \cdot (HSM[i,j] - t_{HSM,j}))]} \quad (8)$$

$$HSM \text{ only : } p_{i,j} = \frac{K_j}{[1 + \exp(-r_{HSM,j} \cdot (HSM[i,j] - t_{HSM,j}))]} \quad (9)$$

$$FSM \text{ only : } p_{i,j} = \frac{K_j}{[1 + \exp(-r_{FSM,j} \cdot (FSM[i,j] - t_{FSM,j}))]} \quad (10)$$

$$None : p_{i,j} = K_j \quad (11)$$

369 Outputs of the model, selection of cold or dry margin, shade and drought tolerance, and respective
 370 competitive dominance index per species All the models fitted are presented in Table S5. Models selection,
 371 margin selection, and parameters estimates are shown in Table S6.

Species	Model	log-likelihood	Divergence	Rhat	AUC	bic
Abies alba	2var	-36862.94	0.02	1.00	0.72	73735.88
Abies alba	hsm	-37206.27	0.02	1.01	0.65	74418.54
Abies alba	fsm	-38536.32	0.01	1.00	0.63	77078.64
Abies alba	none	-38744.63	0.01	1.00	0.50	77491.25
Acer campestre	2var	-25458.98	0.02	1.00	0.59	50927.97
Acer campestre	fsm	-25509.46	0.01	1.00	0.51	51024.92
Acer campestre	none	-26201.90	0.01	1.01	0.50	52405.80
Acer campestre	hsm	-26200.10	0.02	1.00	0.57	52406.21
Acer monspessulanum	fsm	-4470.45	0.01	1.00	0.64	8946.90
Acer monspessulanum	2var	-4477.10	0.02	1.00	0.64	8964.21
Acer monspessulanum	none	-4569.65	0.01	1.00	0.50	9141.30
Acer monspessulanum	hsm	-4603.11	0.01	15.67	0.73	9212.23
Acer platanoides	2var	-11456.06	0.01	21.94	0.50	22922.12
Acer platanoides	hsm	-11469.71	0.01	1.00	0.61	22945.42
Acer platanoides	fsm	-11537.51	0.01	1.01	0.68	23081.02
Acer platanoides	none	-11587.95	0.01	1.00	0.50	23177.89
Acer pseudoplatanus	2var	-44059.69	0.02	1.01	0.72	88129.37
Acer pseudoplatanus	fsm	-45459.75	0.01	1.00	0.51	90925.51
Acer pseudoplatanus	hsm	-45573.20	0.01	1.00	0.60	91152.40
Acer pseudoplatanus	none	-46616.37	0.01	1.00	0.50	93234.75
Alnus glutinosa	hsm	-37296.57	0.02	1.01	0.62	74599.14

<i>Alnus glutinosa</i>	2var	-37297.21	0.02	1.00	0.63	74604.42
<i>Alnus glutinosa</i>	none	-38137.75	0.01	1.00	0.50	76277.51
<i>Alnus glutinosa</i>	fsm	-38145.60	0.01	1.01	0.55	76297.20
<i>Alnus incana</i>	2var	-26455.38	0.02	16.51	0.74	52920.76
<i>Alnus incana</i>	hsm	-26460.08	0.02	1.00	0.73	52926.16
<i>Alnus incana</i>	none	-28171.03	0.01	1.00	0.50	56344.07
<i>Alnus incana</i>	fsm	-28173.07	0.01	30.31	0.83	56352.13
<i>Arbutus unedo</i>	fsm	-7287.22	0.01	1.00	0.83	14580.44
<i>Arbutus unedo</i>	2var	-7304.04	0.02	10.54	0.74	14618.09
<i>Arbutus unedo</i>	none	-8105.40	0.01	1.00	0.50	16212.80
<i>Arbutus unedo</i>	hsm	-8138.85	0.01	16.25	0.72	16283.70
<i>Betula pendula</i>	hsm	-62268.66	0.02	1.00	0.67	124543.33
<i>Betula pendula</i>	2var	-62269.26	0.02	13.00	0.67	124548.53
<i>Betula pendula</i>	none	-65507.65	0.01	1.01	0.50	131017.31
<i>Betula pendula</i>	fsm	-65524.65	0.01	40.46	0.71	131055.30
<i>Betula pubescens</i>	hsm	-72402.90	0.02	1.01	0.74	144811.79
<i>Betula pubescens</i>	none	-77424.99	0.01	1.00	0.50	154851.97
<i>Betula pubescens</i>	2var	-98005.19	0.02	43.39	0.74	196020.37
<i>Betula pubescens</i>	fsm	-103020.95	0.02	50.88	0.50	206047.91
<i>Carpinus betulus</i>	2var	-46552.62	0.02	1.01	0.66	93115.23
<i>Carpinus betulus</i>	fsm	-47442.45	0.01	1.00	0.54	94890.90
<i>Carpinus betulus</i>	hsm	-49219.48	0.01	1.00	0.51	98444.97
<i>Carpinus betulus</i>	none	-49687.76	0.01	1.00	0.50	99377.52
<i>Corylus avellana</i>	2var	-18220.62	0.02	1.00	0.67	36451.23
<i>Corylus avellana</i>	fsm	-18582.52	0.01	1.00	0.57	37171.04
<i>Corylus avellana</i>	hsm	-18744.33	0.01	1.00	0.51	37494.66
<i>Corylus avellana</i>	none	-18877.36	0.01	1.01	0.50	37756.72
<i>Fagus sylvatica</i>	2var	-86640.47	0.02	1.00	0.72	173290.93
<i>Fagus sylvatica</i>	fsm	-93344.50	0.01	2585.45	0.52	186695.00
<i>Fagus sylvatica</i>	hsm	-94739.55	0.01	1.01	0.57	189485.10
<i>Fagus sylvatica</i>	none	-97458.91	0.01	1.00	0.50	194919.82
<i>Fraxinus excelsior</i>	2var	-58020.26	0.01	1.01	0.67	116050.51
<i>Fraxinus excelsior</i>	hsm	-59694.11	0.01	1.01	0.55	119394.23
<i>Fraxinus excelsior</i>	fsm	-59995.22	0.01	1.01	0.54	119996.44
<i>Fraxinus excelsior</i>	none	-60701.41	0.01	1.01	0.50	121404.82
<i>Ilex aquifolium</i>	2var	-7015.03	0.01	1.00	0.75	14040.06
<i>Ilex aquifolium</i>	fsm	-7085.05	0.01	1.00	0.66	14176.10
<i>Ilex aquifolium</i>	hsm	-7479.62	0.01	1.01	0.53	14965.25
<i>Ilex aquifolium</i>	none	-7509.41	0.01	1.01	0.50	15020.83
<i>Juniperus communis</i>	none	-4081.36	0.01	1.00	0.50	8164.72
<i>Juniperus communis</i>	hsm	-4086.15	0.01	2.94	0.55	8178.31
<i>Juniperus communis</i>	fsm	-69529.34	0.91	1.18	0.50	139064.68
<i>Juniperus communis</i>	2var	-69541.64	0.61	7.35	0.55	139093.29
<i>Juniperus thurifera</i>	2var	-9647.11	0.07	12.40	0.71	19304.22
<i>Juniperus thurifera</i>	fsm	-9651.04	0.01	1.00	0.70	19308.08
<i>Juniperus thurifera</i>	hsm	-10623.78	0.48	15.68	0.50	21253.56
<i>Juniperus thurifera</i>	none	-10632.66	0.01	1.00	0.50	21267.32
<i>Larix decidua</i>	2var	-32964.22	0.02	1.00	0.72	65938.44
<i>Larix decidua</i>	hsm	-33633.86	0.01	1.01	0.64	67273.71

Larix decidua	fsm	-34552.84	0.01	193.84	0.65	69111.68
Larix decidua	none	-34872.45	0.01	1.00	0.50	69746.89
Olea europaea	fsm	-4013.43	0.01	1.00	0.91	8032.87
Olea europaea	2var	-4019.66	0.02	1.00	0.91	8049.33
Olea europaea	none	-5053.33	0.01	1.00	0.50	10108.67
Olea europaea	hsm	-5060.54	0.01	1.00	0.76	10127.07
Picea abies	hsm	-120559.95	0.02	1.00	0.75	241125.90
Picea abies	2var	-122373.21	0.02	101.12	0.73	244756.42
Picea abies	none	-137667.82	0.01	1.01	0.50	275337.63
Picea abies	fsm	-138329.83	0.01	788.25	0.85	276665.66
Pinus nigra	fsm	-40121.49	0.01	1.01	0.64	80248.99
Pinus nigra	none	-40736.20	0.01	1.01	0.50	81474.41
Pinus nigra	2var	-41282.28	0.02	553.07	0.49	82574.56
Pinus nigra	hsm	-41327.22	0.01	703.39	0.79	82660.45
Pinus pinaster	fsm	-39247.27	0.02	1.01	0.86	78500.54
Pinus pinaster	2var	-39254.20	0.02	1.00	0.86	78518.40
Pinus pinaster	none	-48718.30	0.01	1.00	0.50	97438.61
Pinus pinaster	hsm	-49300.32	0.01	690.49	0.76	98606.63
Pinus pinea	fsm	-12834.96	0.01	1.00	0.88	25675.92
Pinus pinea	2var	-12842.51	0.02	1.00	0.87	25695.01
Pinus pinea	none	-14510.43	0.01	1.00	0.50	29022.86
Pinus pinea	hsm	-14518.53	0.01	1.00	0.75	29043.06
Pinus sylvestris	hsm	-135220.15	0.02	1.00	0.66	270446.31
Pinus sylvestris	2var	-137240.54	0.02	4.77	0.66	274491.07
Pinus sylvestris	none	-141042.77	0.01	1.01	0.50	282087.55
Pinus sylvestris	fsm	-143079.97	0.01	97.30	0.50	286165.93
Populus alba	fsm	-3669.33	0.70	1.03	0.60	7344.65
Populus alba	2var	-3674.55	0.71	1.03	0.54	7359.10
Populus alba	none	-3763.48	0.01	1.01	0.50	7528.97
Populus alba	hsm	-3769.09	0.01	1.00	0.59	7544.19
Populus nigra	fsm	-11208.10	0.01	1.00	0.46	22422.20
Populus nigra	2var	-11207.23	0.01	1.00	0.46	22424.45
Populus nigra	none	-11285.85	0.01	1.00	0.50	22573.69
Populus nigra	hsm	-11292.40	0.01	1.01	0.59	22590.81
Prunus avium	2var	-24706.00	0.02	1.01	0.65	49422.01
Prunus avium	fsm	-25052.83	0.01	1.00	0.50	50111.66
Prunus avium	hsm	-25701.35	0.01	1.00	0.51	51408.71
Prunus avium	none	-25888.85	0.01	1.00	0.50	51779.71
Prunus padus	hsm	-7037.55	0.01	1.00	0.66	14081.09
Prunus padus	2var	-7052.28	0.01	8.71	0.57	14114.56
Prunus padus	none	-7157.19	0.01	1.01	0.50	14316.39
Prunus padus	fsm	-7192.44	0.01	1.00	0.67	14390.88
Quercus ilex	fsm	-54812.46	0.02	1.00	0.84	109630.92
Quercus ilex	2var	-54828.80	0.83	1.40	0.84	109667.60
Quercus ilex	none	-62989.23	0.01	1.00	0.50	125980.46
Quercus ilex	hsm	-63001.80	0.30	42.45	0.50	126009.61
Quercus petraea	2var	-57105.21	0.02	1.00	0.66	114220.41
Quercus petraea	fsm	-58157.40	0.01	1.00	0.46	116320.81
Quercus petraea	hsm	-59233.85	0.02	1.00	0.51	118473.69

Quercus petraea	none	-59878.23	0.01	1.01	0.50	119758.46
Quercus pubescens	fsm	-34005.55	0.31	172.74	0.50	68017.09
Quercus pubescens	none	-34189.75	0.01	1.01	0.50	68381.51
Quercus pubescens	hsm	-34198.22	0.01	1.00	0.68	68402.45
Quercus pubescens	2var	-34243.05	0.32	197.25	0.68	68496.11
Quercus robur	2var	-84084.66	0.02	1.01	0.67	168179.32
Quercus robur	fsm	-85516.99	0.01	1.00	0.61	171039.99
Quercus robur	hsm	-86672.95	0.02	1.01	0.52	173351.90
Quercus robur	none	-87644.26	0.01	1.00	0.50	175290.52
Quercus suber	fsm	-16824.16	0.21	6.29	0.78	33654.33
Quercus suber	2var	-16826.86	0.02	1.00	0.94	33663.72
Quercus suber	none	-18530.35	0.01	1.00	0.50	37062.70
Quercus suber	hsm	-18605.49	0.21	64.82	0.48	37216.97
Sorbus aria	2var	-11522.36	0.03	1.01	0.62	23054.71
Sorbus aria	fsm	-11557.84	0.01	1.00	0.52	23121.67
Sorbus aria	hsm	-11669.92	0.01	1.00	0.52	23345.84
Sorbus aria	none	-11696.00	0.01	1.01	0.50	23393.99
Sorbus torminalis	fsm	-9093.09	0.11	1.05	0.62	18192.18
Sorbus torminalis	2var	-9095.92	0.08	1.06	0.52	18201.85
Sorbus torminalis	none	-9322.57	0.01	1.00	0.50	18647.13
Sorbus torminalis	hsm	-9327.87	0.02	1.00	0.62	18661.74
Taxus baccata	2var	-2873.67	0.02	1.00	0.73	5757.34
Taxus baccata	fsm	-2887.53	0.01	1.00	0.69	5781.06
Taxus baccata	hsm	-2980.96	0.01	1.00	0.51	5967.92
Taxus baccata	none	-2986.14	0.01	1.00	0.50	5974.28
Tilia cordata	hsm	-14332.10	0.01	1.01	0.55	28670.19
Tilia cordata	none	-14487.85	0.01	1.00	0.50	28977.70
Tilia cordata	2var	-15005.13	0.02	1.00	0.60	30020.26
Tilia cordata	fsm	-15172.12	0.30	4.00	0.50	30350.23
Tilia platyphyllos	2var	-6602.28	0.01	1.00	0.61	13214.57
Tilia platyphyllos	fsm	-6631.70	0.01	1.00	0.56	13269.41
Tilia platyphyllos	hsm	-6678.97	0.01	1.01	0.53	13363.93
Tilia platyphyllos	none	-6699.23	0.01	1.00	0.50	13400.45

Table 5: Model and indicator computed for the four model fitted by species

Species	n	Model	prevalence	k_int	r_fsm	t_fsm	r_hsm	t_hsm	I_fsm	I_hsm	Data FSM	Data HSM
Abies alba	9382	2var	0.01	0.08	0.21	0.49	1.23	2.74	99.79	35.05	TRUE	TRUE
Acer campestre	5781	2var	0.05	0.04	1.56	1.89	0.28	-0.08	100.00	43.36	TRUE	TRUE
Acer monspessulanum	716	fsm	0.01	0.00	0.25	0.12			99.53		TRUE	TRUE
Acer platanoides	2096	hsm	0.02	0.01			0.49	0.22		70.60	TRUE	TRUE
Acer pseudoplatanus	12412	2var	0.10	0.10	1.53	3.33	0.67	1.81	100.00	41.12	TRUE	TRUE
Alnus glutinosa	9781	hsm	0.05	0.08			0.50	0.43		8.17	TRUE	TRUE
Alnus incana	6562	hsm	0.06	0.09			1.64	1.43		0.02	FALSE	TRUE
Arbutus unedo	1673	fsm	0.03	0.01	1.28	0.67			100.00		TRUE	FALSE
Betula pendula	20558	hsm	0.11	0.22			0.80	1.79		0.59	TRUE	TRUE
Betula pubescens	26676	hsm	0.14	0.32			0.95	1.98		0.00	FALSE	TRUE
Carpinus betulus	13224	2var	0.17	0.10	1.43	-1.81	0.51	0.92	100.00	60.87	TRUE	TRUE
Corylus avellana	3923	2var	0.02	0.04	0.22	-0.14	0.52	0.15	94.10	32.09	TRUE	TRUE
Fagus sylvatica	35853	2var	0.32	0.36	1.77	3.62	0.59	2.52	100.00	17.92	TRUE	TRUE
Fraxinus excelsior	17889	2var	0.11	0.17	0.28	-2.32	0.60	1.93	98.93	39.38	TRUE	TRUE
Ilex aquifolium	1250	2var	0.01	0.01	1.06	0.33	0.46	0.14	100.00	79.02	TRUE	TRUE
Juniperus communis	658	none	0.00	0.00	0.00	0.00	0.00	0.00	0.00	0.00	TRUE	TRUE
Juniperus thurifera	1858	fsm	0.12	0.01	1.49	0.94			100.00			
Larix decidua	8204	2var	0.24	0.07	0.92	1.36	1.09	2.13	100.00	38.86		
Olea europaea	1274	fsm	0.02	0.03	0.47	0.13			27.17		TRUE	FALSE
Picea abies	70302	hsm	0.46	0.91			1.01	3.67		0.00	FALSE	TRUE
Pinus nigra	10652	fsm	0.21	0.05	0.07	0.32			79.44		TRUE	TRUE
Pinus pinaster	16500	fsm	0.35	0.14	0.81	4.89			99.96		TRUE	FALSE
Pinus pinea	4373	fsm	0.10	0.02	0.80	1.65			100.00		TRUE	FALSE
Pinus sylvestris	75719	hsm	0.39	0.60			0.39	1.76		7.46	FALSE	TRUE
Populus alba	588	none	0.00	0.00	0.00	0.00	0.00	0.00	0.00	0.00	TRUE	FALSE
Populus nigra	2121	fsm	0.01	0.02	0.16	-0.25			76.80		TRUE	TRUE
Prunus avium	5650	2var	0.04	0.04	0.92	-1.22	0.50	0.57	100.00	72.39	TRUE	TRUE
Prunus padus	1214	hsm	0.01	0.01			0.72	0.26		76.55	FALSE	TRUE
Quercus ilex	22661	fsm	0.28	0.15	0.74	7.09			100.00		TRUE	FALSE
Quercus petraea	17116	2var	0.14	0.12	3.26	5.68	0.52	1.31	100.00	67.54	TRUE	TRUE
Quercus pubescens	8522	none	0.14	0.03	0.00	0.00	0.00	0.00	0.00	0.00	TRUE	TRUE
Quercus robur	31078	2var	0.22	0.20	1.14	6.90	0.43	1.32	100.00	53.75	TRUE	TRUE
Quercus suber	5975	2var	0.23	0.05	0.31	1.81	0.00	0.00	98.08	0.00	TRUE	FALSE
Sorbus aria	2113	2var	0.01	0.01	0.31	0.23	0.32	0.05	99.97	72.58	TRUE	TRUE
Sorbus torminalis	1613	2var	0.02	0.01	4.66	0.47	0.07	-0.01	100.00	5.78	TRUE	TRUE
Taxus baccata	434	2var	0.11	0.00	0.50	0.06	0.53	0.02	99.99	89.36		
Tilia cordata	2718	hsm	0.02	0.02			0.49	0.16		53.38	TRUE	TRUE
Tilia platyphyllos	1078	2var	0.01	0.01	0.35	0.13	0.33	-0.00	99.99	31.66	TRUE	TRUE

Table 6: Model outputs

372 7 Generic model and transferability

373 As the generic model was calibrated on all species, the fit time was much longer. To overcome this, we
 374 aggregated the presence data to the resolution of the climatic data (each climatic data cell could include
 375 up to 81 occurrence data cells). We then fitted a binomial model in which the number of successes
 376 corresponded to the number of presence events observed in each climate cell, and the probability of
 377 success was modelled by the equation 6. We used the same priors for parameters r and t as for the specific
 378 models. The random effect on the K_{sp} asymptote was modeled with a beta distribution, parameterized
 379 so that K is the mean and λ is a scaling parameter. We used a beta law with parameters 1.5 and 15 as
 380 a prior for K , and a gamma law with a shape parameter of 18 and an intensity parameter of 0.5. The
 381 table 7 presents the quality metrics for predicting species distributions using a generic model.

species	tss	specificity	sensitivity	auc
Acer pseudoplatanus	0.43	0.59	0.85	0.75
Betula pubescens	0.24	0.79	0.46	0.68
Carpinus betulus	0.34	0.40	0.94	0.66
Fagus sylvatica	0.47	0.65	0.83	0.77
Fraxinus excelsior	0.28	0.39	0.89	0.69
Ilex aquifolium	0.48	0.58	0.90	0.78
Picea abies	0.01	0.02	0.99	0.67
Pinus pinea	0.29	0.49	0.80	0.65
Prunus padus	0.11	0.18	0.94	0.47
Quercus petraea	0.33	0.52	0.81	0.68
Quercus suber	0.22	0.44	0.78	0.61
Sorbus aria	0.26	0.49	0.77	0.65
Tilia cordata	0.11	0.22	0.89	0.55
Abies alba	0.38	0.57	0.80	0.72
Acer campestre	0.30	0.47	0.84	0.65
Acer monspessulanum	0.16	0.25	0.91	0.54
Acer platanoides	0.27	0.48	0.79	0.64
Alnus glutinosa	0.14	0.19	0.94	0.56
Alnus incana	0.23	0.53	0.70	0.62
Arbutus unedo	0.44	0.58	0.86	0.74
Corylus avellana	0.31	0.67	0.64	0.69
Juniperus thurifera	0.61	0.67	0.94	0.77
Larix decidua	0.39	0.56	0.82	0.71
Olea europaea	0.63	0.77	0.86	0.86
Pinus pinaster	0.41	0.60	0.82	0.72
Populus alba	0.16	0.41	0.74	0.59
Populus nigra	0.31	0.39	0.92	0.63
Prunus avium	0.33	0.39	0.94	0.69
Quercus robur	0.26	0.51	0.76	0.67
Taxus baccata	0.43	0.62	0.81	0.77
Tilia platyphyllos	0.23	0.41	0.82	0.62

Table 7: Metrics of predictions quality for assessing model transferability

382 8 Supplementary result figures

383 8.1 Correlation between percentiles of climatic variables and maximum ex- 384 perienced stress

385 The figure S7 show the pair plots and correlation between the percentiles of the climatic variables and
 386 maximum experienced stress. We represent the 5th percentiles for *map*, *map-pet*, *mat*, Ψ_{min} and T_{min} ,
 387 and the 95th percentiles for *pet*, as explained in the main text.

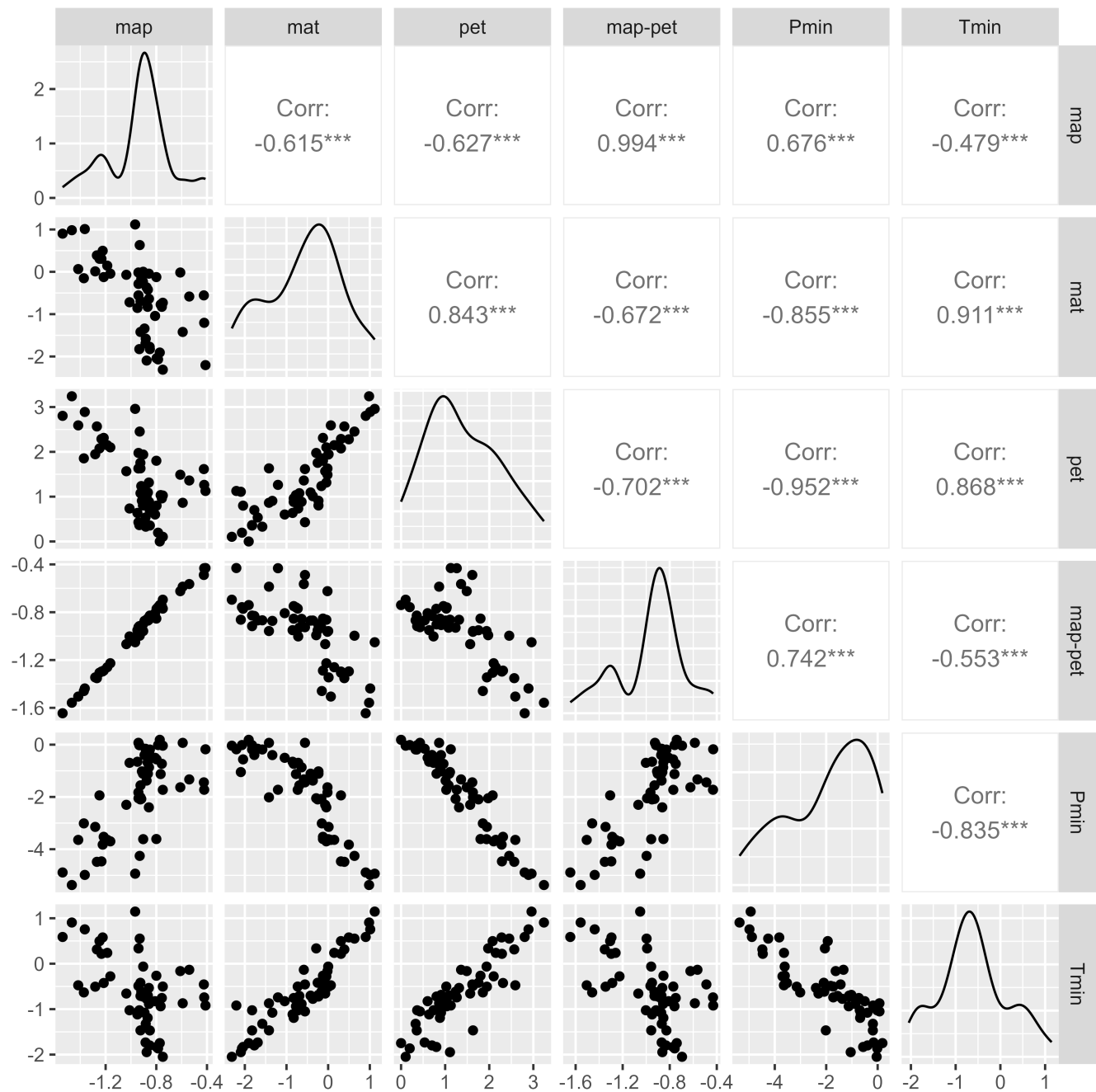


Figure 7: Pairplots and correlations between percentiles of climatic variables and maximum experienced stress. Lower diagonal pannels represent scatter plot, diagonal pannels are density of each variables, and in upper diagonal pannels written the Pearson's correlation and their significance. *, **, or ***, correspond respectively to p-value less than 0.05, 0.01 and 0.001.

388 **8.2 Correlation between maximum experienced stress and frost and drought
389 tolerance traits**

390 On the figures S8 and S9 are presented the scatter plot which effect size are presented in the Results—
391 Fig. 2. Each points represent a species.

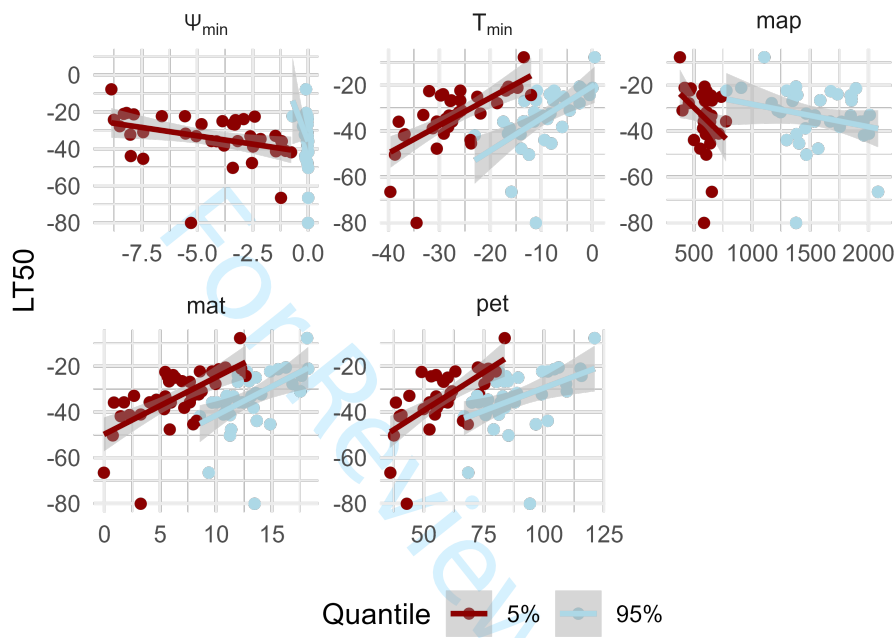


Figure 8: Regression plot of LT_{50} against climatic niche extremes. The climatic niche extreme is estimated using 5th and 95th percentiles of climatic variables (mean annual precipitation *map*, mean annual temperature *mat*, annual potential evapotranspiration *pet*) or maximum experienced stress (minimum temperature T_{min} and minimum soil potential Ψ_{min}). The analysis includes all species for which the occurrence data cover the corresponding margin of the distribution (see Methods for details). We overlayed linear models and their confidence intervals.

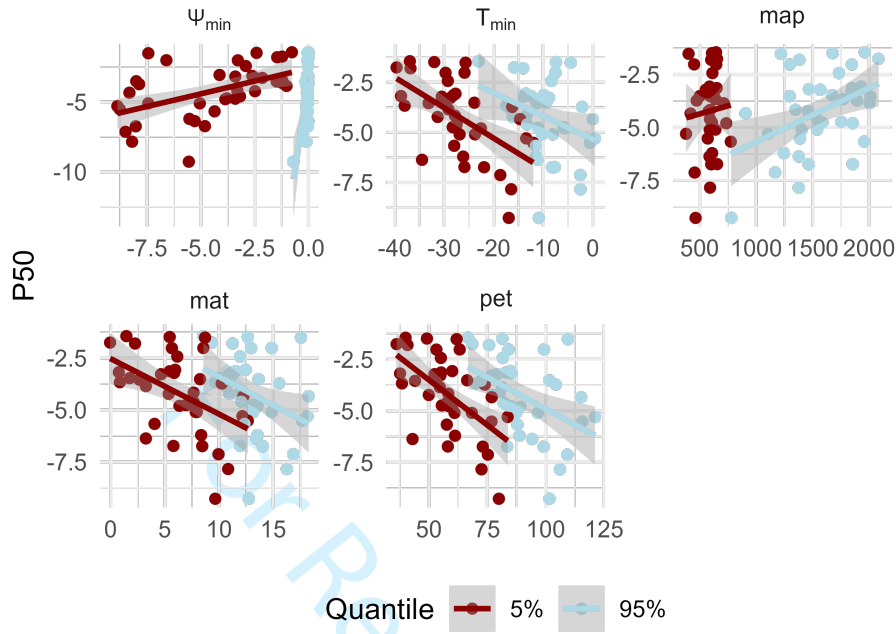


Figure 9: Regression plot of Ψ_{50} against climatic niche extremes. The climatic niche extreme is estimated using 5th and 95th percentiles of climatic variables (mean annual precipitation *map*, mean annual temperature *mat*, annual potential evapotranspiration *pet*) or maximum experienced stress (minimum temperature T_{min} and minimum soil potential Ψ_{min}). The analysis includes all species for which the occurrence data cover the corresponding margin of the distribution (see Methods for details). We overlayed linear models and their confidence intervals.

8.3 Competitive dominance effect on the link between probability of presence and safety margin?

On the figure S?? are displayed the result of the standardized linear regression which results are presented in the Results.

Effects of competitive dominance index on model metrics.

392 References

- 393 Charra-Vaskou, K., G. Charrier, R. Wortemann, B. Beikircher, H. Cochard, et al. (2012). Drought and
394 frost resistance of trees: a comparison of four species at different sites and altitudes. *Annals of Forest
395 Science* 69.3, pp. 325–333. DOI: 10.1007/s13595-011-0160-5.
- 396 Charrier, G., H. Cochard, and T. Ameglio (2013). Evaluation of the impact of frost resistances on potential
397 altitudinal limit of trees. *Tree Physiology* 33.9, pp. 891–902. DOI: 10.1093/treephys/tpt062.
- 398 Cochard, H. (2002). A technique for measuring xylem hydraulic conductance under high negative pres-
399 sures. *Plant, Cell and Environment* 25.6, pp. 815–819. DOI: 10.1046/j.1365-3040.2002.00863.x.
- 400 — (2006). Nucleation/Nucléation Cavitation in trees. *C. R. Physique* 7, pp. 1018–1026. DOI: 10.1016/
401 j.crhy.2006.10.012.
- 402 Delzon, S., C. Douthe, A. Sala, and H. Cochard (2010). Mechanism of water-stress induced cavitation in
403 conifers: bordered pit structure and function support the hypothesis of seal capillary-seeding. *Plant,
404 Cell & Environment* 33.12, pp. 2101–2111. DOI: 10.1111/j.1365-3040.2010.02208.x.
- 405 Hiederer, R. (2013). *Mapping Soil Properties for Europe - Spatial Representation of Soil Database At-
406 tributes*, p. 47.
- 407 Jackson, A. R. B., J. Canadell, J. R. Ehleringer, H. A. Mooney, O. E. Sala, et al. (1996). A Global
408 Analysis of Root Distributions for Terrestrial Biomes. 108.3, pp. 389–411.
- 409 Kollas, C., C. Körner, and C. F. Randin (2014). Spring frost and growing season length co-control the
410 cold range limits of broad-leaved trees. *Journal of Biogeography* 41.4. Ed. by O. Vetaas, pp. 773–783.
411 DOI: 10.1111/jbi.12238.
- 412 Lenz, A., G. Hoch, Y. Vitasse, and C. Körner (2013). European deciduous trees exhibit similar safety
413 margins against damage by spring freeze events along elevational gradients. *New Phytologist* 200.4,
414 pp. 1166–1175. DOI: 10.1111/nph.12452.
- 415 Leuschner, C. and I. C. Meier (2018). The ecology of Central European tree species: Trait spectra, func-
416 tional trade-offs, and ecological classification of adult trees. *Perspectives in Plant Ecology, Evolution
417 and Systematics* 33, pp. 89–103. DOI: 10.1016/j.ppees.2018.05.003.
- 418 Martin-StPaul, N., S. Delzon, and H. Cochard (2017). Plant resistance to drought depends on timely
419 stomatal closure. *Ecology Letters* 20.11. Ed. by H. Maherli, pp. 1437–1447. DOI: 10.1111/ele.12851.
- 420 Olson, D. M., E. Dinerstein, E. D. Wikramanayake, N. D. Burgess, G. V. Powell, et al. (2001). Terrestrial
421 ecoregions of the world: A new map of life on Earth. *BioScience* 51.11, pp. 933–938. DOI: 10.1641.
422 0006-3568.
- 423 Pammenter, N. W. and C. Van der Willigen (1998). A mathematical and statistical analysis of the
424 curves illustrating vulnerability of xylem to cavitation. *Tree Physiology* 18.8-9, pp. 589–593. DOI:
425 10.1093/treephys/18.8-9.589.
- 426 Schulzweida, U. (2022). *CDO User Guide*. DOI: 10.5281/zenodo.7112925.
- 427 Sperry, J. S., F. R. Adler, G. S. Campbell, and J. P. Comastock (1998). Limitation of plant water use by
428 rhizosphere and xylem conductance: results from a model. *Plant Cell and Environment* 21, pp. 347–
429 359.
- 430 Tóth, B., M. Weynans, L. Pásztor, and T. Hengl (2017). 3D soil hydraulic database of Europe at 250 m
431 resolution. *Hydrological Processes* 31.14, pp. 2662–2666. DOI: 10.1002/HYP.11203.
- 432 Van Genuchten, M. T. (1980). A Closed-form Equation for Predicting the Hydraulic Conductivity of
433 Unsaturated Soils. *Soil science society of america* 44, pp. 892–899.
- 434 Vitra, A., A. Lenz, and Y. Vitasse (2017). Frost hardening and dehardening potential in temperate trees
435 from winter to budburst. *New Phytologist* 216.1, pp. 113–123. DOI: 10.1111/nph.14698.

Ecography - revisions

Recommendation by the Subject Editor (Dr. Carissa Brown):

I am recommending your manuscript undergo minor revisions based on the reviews, below. I encourage you to pay particular attention to Reviewer 1's recommendation that you extend your analyses and discussion of the relationship between shade tolerance and physiological limits of species, or to remove that component of the study. R1 gives further suggestions in their detailed review on how you might address those issues. R2 also gives many detailed suggestions on how to improve the accessibility of your work. I encourage you to consider all of their suggestions, and look forward to your revised manuscript.

We are thankful to Dr Carissa Brown for her positive comments and advice. We have addressed the editor's and reviewer's main concerns by removing the competition analysis from the study. We have also carefully considered all reviewer's minor comments to improve the manuscript. The various changes we have made to the manuscript are detailed below.

Reviewer(s)' Comments to Author:

Reviewer: 1

Comments to the Author

This paper applies functional traits of woody-plant species in Europe to estimate their physiological limits in relation to drought and freezing stress. Then, authors use this information in correlative species distribution models to test whether physiological limits are informative on species range distributions. Authors find that hydraulic and frost safety margins are useful traits to inform on species distribution models, which can help in modelling species distributions without the need to use occurrences. These results contribute to close the gap between correlative models and process-based models by using a methodology that can be widely applicable. I find the paper interesting and timely; results are solid and can be of great interest for the community.

The only issue I find is in relation to results on the relationship between species shade tolerance and their physiological limits. Even if the hypothesis on competition for light is interesting, it is addressed in a rather simplistic way. This leads authors to present their results in a very sceptic way, which contrasts with the rest of the results shown. Therefore, I feel that these results need to be complemented by more analyses or, if convenient, dropped from the current paper, as they are not central to the story. Some complementary analyses I propose for authors, if they want to keep this part of the story, would be to use continuous traits related to light competition such as tree height to see whether it relates to the physiological limits of species. Height could be used also in a site-specific way to calculate an index of species- and site-specific height relative to the maximum height of the site. However, these are only some suggestions, so I am not asking authors to perform these extra analyses.

We thank the reviewer for their positive comments and understand their concerns about the analysis of shade tolerance and physiological limits. Despite the reviewer's sensible suggestions of using species maximum height instead of shade tolerance, we have preferred to remove the analysis from the paper. We believe that the aggregated and static data used in this study do not allow us to assess competition with sufficient precision to answer the question. Furthermore, competition is known to be related to multiple traits (see Kraft et al. 2015 PNAS), and many may be tested to represent trees' competitive ability (maximum height, shade tolerance, maximum growth rate, etc.). For a convincing analysis, it would require testing several of them and probably use dynamic data rather than static data on species presence absence. Such analysis is clearly outside the scope of the manuscript and would dilute the main message of the paper.

We also thank the reviewer for their other comments which are very relevant, and that we tried to address in detail hereafter.

Other than that, I have some minor comments (see below).

L7. Please specify which type of models are authors referring to. It can be earth system models, species distribution models, etc. They specify it in the next sentence but I think it would be good to state it from the beginning.

We changed the text accordingly.

L7 : “Species distribution models are key...”

L12. There are some cases where physiological processes are considered in correlative species distribution models. I would try to rephrase the word “failed” so it does not undermine previous work. E.g., Benito-Garzón (2018), cited in the paper.

We changed the word “fail” to “struggle”.

L11-13 : Some correlative species distribution models have tried to include traits but so far have struggled to directly connect to ecophysiological processes.

L13. Not clear what authors mean by “intermediate”.

We changed ‘intermediate strategy’ to “bridging strategy”/“hybrid”

L13 : “Here, we propose a new strategy in which species distributions are”

L118. For a up-to-date global analysis on P50 relationship with climate see Sanchez-Martinez, P., Martínez-Vilalta, J., Dexter, K. G., Segovia, R. A., & Mencuccini, M. (2020). Adaptation and coordinated evolution of plant hydraulic traits. Ecology Letters, 23(11), 1599–1610. <https://doi.org/10.1111/ele.13584>

Great paper, thank you! We added this reference in the text.

L116-119: Some studies have also reported correlations between Ψ50 or LT50 and species mean climate or rough indicators of species climatic range limits (Charrier et al., 2013; Larter et al., 2017; Sanchez-Martinez et al., 2020; Skelton et al., 2021)

L349-350. It would be good to know how climatic variables and climatic niche extremes are correlated.

We tested for the correlations between all the climatic niche extremes and present pairplots in Supplementary Information.

We also mentioned it in the main text.

L357-359 : We also investigated correlations between all the climatic niche extremes and found correlations greater than 0.9 between Ψ_{\min} and pet, and between T_{\min} and mat (see details in Fig. S7)

L352. Please indicate whether this are confidence intervals. Also, I would recommend to use an easier to read numbers when presenting p-values (e.g., $p < 0.001$).

We clarified that intervals referred to 95% confidence intervals and simplified p-values.

L344-347 : For Ψ_{crit} , we observed that the minimum soil potential extreme (i.e. 5th percentile of Ψ_{\min}) has the strongest effect (standardised regression coefficient and its 95% confidence interval: 0.77 [0.29, 1.24]; $p < 0.01$; Fig.2).

L359-361. Does this effect refer to LT50? If so, please indicate it so it is clearer.

Yes, we clarified it.

L353 : "For LT50, we observed an equivalent effect..."

Figure 2. please indicate what the bars show (95% Confidence interval?) and why MAP and P_{\min} do not have them.

We updated the figure so that confidence intervals are more visible, and added information in the caption.

Fig 2 caption : " Bars indicate 95% confidence intervals."

L389. If I understood correctly, FSM show a stronger non-linearity than HSM. If so, please correct the text, which now reads as it is the opposite.

We are sorry for this confusing typo.

L388-389 : The inflection index I for FSM (Fig. 3B) was 10 times higher than for HSM, showing a stronger non-linearity compared to HSM (Fig. 3A).

Figure 3. Please indicate the Y axis name. I would also recommend to use two rows in this figure, curves in the first row and boxplots in the second one, for a better separation and visualization of results.

We added the Y axis name and changed the figure as suggested by the reviewer.

392. Maybe authors are being a bit generous saying that it is a good predictive ability with an $AUC < 0.7$.

We changed "good" to "moderate".

L392 : With a generic model based on safety margins, we found moderate predictive ability for a species not included in the model fit, i.e. "unobserved species".

399. "assumed" or "hypothesized"?

This result was removed.

401. "indeed" or something like "if so"?

This result was removed.

414-415. It would be good to see how these values compare. What AUC do previous studies provide for these species? Just mentioning them in the text (or at least mean and deviation) would be enough to see how they compare to the proposed methodology. Including them in one of the supplementary tables could also be an option.

We added the values found in Vesk et al., 2021 in the result and in the discussion. We couldn't compare species to species, as their study was performed on Eucalypt taxa.

L395-396 : This was close to AUC found for traits-SDM models (AUC median and inter-quartile of Vesk et al. (2021) : 0.65 [0.57,0.77]).

L516-519 : Indeed, we found that when trying to predict the distribution of a species without presence/absence calibration data, our generic models based on safety margins gave AUC ranges similar to trait-SDMs (AUC median and inter-quartile of Vesk et al., 2021 : 0.65 [0.57,0.77])

429-430. But authors do show a moisture effect when looking at the minimum water potential in the soil. I wonder whether this precipitation result would change if you would consider precipitation of the driest quarter (or month). Authors do not need to include these analyses, but at least discuss this possibility. Also, I think that drought duration (and also time exposed to freezing temperatures) may be an important factor to discuss here, as authors do not consider the duration or frequency of extreme climates in the current study, but may be crucial parameters shaping species distributions.

We agree with the reviewer's suggestion and added two paragraphs in the discussion accordingly.

L428-430 : Other more complex variables (such as the precipitation in the driest months) could also have been tested to explain variations in Ψ_{50} , but here we focused on the most classical variables.

L525-530 : The challenge of our safety margin approach is to find a good compromise in the simplification of physiological processes. Too much detail would lead to the complexity pitfalls of mechanistic models, while too much simplicity would produce indicators that are too coarse. For instance, it would be interesting to account for the duration and frequency of negative safety margins. The duration of drought stress is indeed important (Martin-StPaul et al., 2017), but remains difficult to include in safety margins.

431-436. I think that a bit more of discussion related to the frost tolerance traits is needed here. What is the present study bringing into the table compared to these previously mentioned studies looking at frost tolerance?

We emphasized more the novelty of our study on this particular point, which relies on the fact that LT50 is a trait difficult to measure in a standardized way (as it strongly varies with phenology, and therefore to gather for numerous species. Previous studies focused on few species or used heterogeneous sets of traits. Here propose to standardize the trait using winter maximum LT50.

L436-438: A key advance of our study is to show that winter maximum frost hardiness is useful to standardise LT50 extracted from the literature for numerous species and capture species' distribution low-temperature limit.

469. "Among" instead of "between"?

As we are referring to two distinct groups we kept "between".

501. Or to inform occurrence selection and grouping using genetic groups with different sensitivity to climatic extremes (see, for instance, Sanchez-Martinez, P., Marcer, A., Mayol, M. & Riba, M. *Shaping the niche of Taxus baccata, a modelling exercise using biologically meaningful information*. *For. Ecol. Manag.* 501, 119688 (2021)).

Although the study mentioned is of much interest, we believe it would dilute the message in this paragraph, and lengthen the discussion.

524-528. As pointed above, this sentence brings me to the conclusion that results on competitive dominance are not believed by authors. I would rather improve their discussion, complement there results or consider dropping them from the story.

This part of the discussion was removed because the associated result was removed.

544. Please ignore if not pertinent, but I am not familiarized with this wording “crude”, consider revising.

This part of the discussion was removed as explained above.

Reviewer: 2

Comments to the Author

Reviewer report on ECOG-07528 *Living on the edge - physiological tolerance to frost and drought explains range limits of 35 European tree species*

This ms reports on a strategy for modelling tree species distributions that would be useful for understanding and forecasting effects of climate change. The work here proposes a modelling strategy attempting to solve the problems of a lack of ecophysiology in correlative species distribution modelling, on the one hand, and mechanistic models that are highly complex with onerous parameterisation requirements, on the other.

The authors address 4 research questions for 38 tree species across European forests, seeking to explain and predict cold and dry range margins. The authors propose to do this by calculating climatic safety margins for species across space. This is done by obtaining physiological tolerance thresholds for drought and for cold. These are species physiological traits that define a critical threshold response. (By the way, authors might want to read Kearney et al 2021 DOI: 10.1111/1365-2435.13829 for a useful discussion of definition of functional traits that is useful in this paper.) This is contrasted with the, far more widespread, practice of traits defined as physiological (rates) or morphological characters to capture aspects of plant strategies that influence performance (in some unspecified way). The point is this ms's definition of functional trait is highly specific to the proposed challenge of modelling responses to stresses of drought or cold temperatures.

The authors then calculate a series of climatic measures for each site or grid cell. Critically the ones they propose are indices of maximum expected stress (minimum temperature or minimum expected water potential. These are in the same units as the species physiological tolerance thresholds. Which enable the calculation for each species j at each site i the difference between the critical tolerance threshold and the expected maximum climatic stress, which they defines as the safety margin. This is a critical step, because the variables now considered at a site are transformed to be a property of the species in focus. In Kearney's 2006 paper (<https://doi.org/10.1111/j.2006.0030-1299.14908.x>) the environment is defined by

the organisms experience of the world around it. This is an important conceptual point. In most modelling, the factors (conditions and resources) that are used as inputs are regarded without regard to the specific organism—they are generic for a taxonomic/functional group under consideration. One does not typically redefine soil moisture for each new species, for example. Yet that is precisely what is proposed in this study. I don't mean to labour the point, but I feel this is a significant contribution of this work. One that challenges the practice of species distribution modelling more widely.

In sum I think this is a really valuable contribution that has forced me to think deeply. I felt the work well conceived, well executed and well written. I have a few general comments and a number of specific ones. These are all aimed at aiding the accessibility and impact of the work. Best wishes with your work and, no, I am not Mike Kearney.

We thank the reviewer for their positive comments and suggestions to improve our work. We corrected our work as suggested by the reviewer and detailed it hereafter.

L260, I found the explanation of the treatment of range edges by considering percentiles of the distribution and the expert-derived distributions from EuForgen quite confusing. See L260 and Supplement SI5 comments.

We simplified the text in the methods and clarified the details in supplementary materials.

L249-256 : For each species, we determined whether the presence/absence EuForest dataset captured its distribution limit at the dry or cold margin. For instance, EuForest captures the dry margin of a species if it includes absence observations in dryer locations than the margin of the species. If this is not the case, it is not possible to tell whether the dry margin in EuForest data is an environmental margin or the limit of the dataset. We tested the coverage of each margin by comparing the 95th percentile of pet and the 5th percentile of mat between the presence and absence of each species (see details in SI5). We tested the drop in the probability of presence only for the margins covered by the EuForest data

SI, L399-411: For each species, we checked whether occurrence data enabled to cover the distribution limit at its cold and dry margin. Figure S6 details how we perform this analysis and gives an example of a species for which the cold margin is not well covered, but the dry margin is. For the cold margin, we computed the 5th percentiles of mat over all the absences falling outside the distribution and over the occurrence (absence or presence) falling inside the expert-based EuForgen distribution. Note we took all the occurrences inside EuForgen for computing percentiles of the species distribution, to deal with species that would have very low prevalence and for which percentiles would not represent well the limit of the expert map. If the 5th percentile of absences was below the 5th percentile of inside occurrences, then the distribution limit at the cold margin was covered by the EuForest data. The approach was the same with the dry margin, using 95th percentiles of pet. The table S6 summarises for each species whether the margin could be tested or not (column "Cold margin" and "Dry margin", TRUE/FALSE).

L270 how was performance measured r^2 ? Larger/tighter estimated effect sizes?

We specified in the text that we were using R² and effect-size.

L267-270 : R² of the regression and effect-size (computed as standardised coefficients, see Schielzeth, 2010) were used to quantify the strength of the relation between climatic niche extremes and species physiological tolerance traits.

L281ff Equation 6 presents the model as a product of two logistic functions against a max Probability of presence. Importantly FSM and HSM are species-specific. i.e. the environment depends upon the species. This is conceptually sensible, but it is not comparable with covariates that are measured without regard to the species. More a comment, and pointing out that this could be emphasised.

Here and elsewhere, you use a subscript index i to reflect site or gridcell i , I think. But you do not index the species as subscript j , as most SDM modellers might expect. If you are to use a superscripts for species, which is an unconventional notation in ecology (though more widely used in maths), you should be more clear about this. p_i needs to be indexed by species.

Also, it is worth stating whether the model has any free parameters to be estimated from the data (k, r, t ?). It is worth being explicit about this. And if so, I would expect they be reported with estimated error. (Table 5)

We thank the reviewer for their attention to details, and corrected the formalism of our equations accordingly.

We updated equation 6 as follow :

$$p_{i,j} = \frac{K_j}{[1 + \exp(-r_{FSM,j} \cdot (FSM[i,j] - t_{FSM,j}))] \cdot [1 + \exp(-r_{HSM,j} \cdot (HSM[i,j] - t_{HSM,j}))]}$$

L281 : with $t_{FSM,j}$, $r_{FSM,j}$ and K_j being model estimated parameters, j the species and i a grid cell.

And equation 7,8:

$$p_{i,j} = \frac{K_j}{[1 + \exp(-r_{FSM} \cdot (FSM[i,j] - t_{FSM}))] \cdot [1 + \exp(-r_{HSM} \cdot (HSM[i,j] - t_{HSM}))]} \\ K_j \sim \mathcal{B}(\lambda \cdot K, \lambda \cdot (1 - K))$$

L330 : with $t_{FSM,j}$, $r_{FSM,j}$, K_j , K and λ being model estimated parameters, j the species and i a grid cell.

L309 I don't see the results of this. Did you only accept a better BIC if it was >2 BIC units lower than the next best model? Basically, how did you decide? Additionally, one might expect a measure of fit, like deviance.

We added a table with all the models fitted, and their RHat, percentage of divergent transitions, log-likelihood and BIC in the supplementary material. We also clarified that model selection was based on BIC being 2 units lower than next best model (the difference was always greater than 2). We used AUC as a measure of fit, when AUC was computed on the fit dataset, and as a measure of quality of predictions when it was calculated on the occurrence of a species not included in the fit.

L307-314: Then, for each species, we selected the model with the lowest Bayesian Information Criterion - BIC (Schwarz, 1978) among the converging models. The difference in BIC with the next best model was always greater than 2 indicating strong support for the selected model (see Table S5)

We computed AUC (Fielding and Bell, 1997) for each model using the model predictions over the data used in the fit. AUC measures the fit quality, 0.5 being the AUC of a random model and 1 of a perfect fit.

SI : All the models fitted are presented in Table S5. Models selection, margin selection, and parameters estimates are shown in Table S6.

L322 I welcome this internal cross validation but note (leave-one-species out) is always optimistic compared to external cross validation.

We agree with the reviewer that external validation would be a stronger evaluation of the models' predictive abilities. This would require presence/absence data covering the distributions of a distinct species pool (for instance for North America) and to be able to compute the safety margins over their distributions (based on Pmin and Tmin). This would be a large task and at the time of our study, some variables needed to compute Pmin in other continents were missing. We however mentioned the importance of external cross-validation in discussion.

L519-520 : It would be interesting to also test the predictive ability of our model in new continents or regions with a distinct species pool as in Vesk et al. (2021).

Fig 2. In left panel, is Psi crit = Psi_50? Please check for consistency.

Psi_crit refers to either P50 or P88 depending of the species being a gymnosperm or an angiosperm. This is mentioned in the methods, but we added it in the figure caption to avoid any confusion.

Fig 2 cation : Ψ_{crit} refers to Ψ_{50} (gymnosperms) or Ψ_{88} (angiosperms).

L364 ff. it is not clear that selection of the predictor variable means 'explained'. As far as I can tell you report no measure of fit. And the model selection does not include other alternative predictors. So I felt this needed a bit more evidence.

We added in the results the values of AUC computed and changed the title of this result.

L371-375 : The mean AUC of all models was 0.69, with 25 species having AUC over 0.65 indicating acceptable fits, and six of which had particularly good fits with AUC over 0.8. The ten other species had low AUC (<0.65) which may be caused by their very low prevalence (median prevalence and quartiles of these 10 species : 0.017 [0.013,0.04] contrasts with the 25 other species: 0.11 [0.04,0.22]).

L421 To be fair, what are called classical climate variables are used because they are convenient and often highly correlated with climatic extremes. And there are many papers which point out that extremes may be more useful and powerful, see e.g.

<https://doi.org/10.1111/ecog.05253>.

We added a sentence on this matter.

LX : This is consistent with recent studies that have emphasised the importance of using climatic extremes rather than averages to explain ecological patterns, despite being well correlated (Stewart et al., 2021)

L427, again the issue with what this means. You haven't defined or measured explanation. We now explain in the methods section that R2 and effect-size were taken as measures of explanation. We changed the text accordingly here.

L267-270 : R2 of the regression and effect-size (computed as standardised coefficients, see Schielzeth, 2010) were used to quantify the strength of the relation between climatic niche extremes and species physiological tolerance traits.

L425-427 : Larter et al. (2017) and Skelton et al. (2021) reported that species with lower mean *map* were found to have greater resistance to embolism, whereas we found no significant relationship between P50 and *map* percentiles.

L516 suggest “to” for “than for”

Ok

L524, but also the use of P/A data at a 1km2 resolution.

We removed this part of the discussion

SI5 L402, do these percentiles refer to all points (presence & absence)? Or only presences? L404 for “distribution”, do you mean the EuForGen distribution?

Fig S6 confuses me. Shouldn’t the mat example on bottom panel be making reference to 5th percentiles (not 95th). Conversely, shouldn’t the pet analysis in the upper panel make reference to the 95th percentile? And now I am quite confused by the protocol for decision about whether thresholds can be used. Please read carefully and revise this whole section. We acknowledge this section was unclear, and clarify the text in the main methods (see above) and in the SI. We also corrected the figure where we mistakenly swapped the two variables, as the reviewer mentioned.

SI, L399-411 (cited above)

Table 5, n is and integer. No decimal places

We removed the decimals.

Table 6 indicates much higher sensitivity than specificity.

This implies the model correctly identifies presences much better than it is at correctly identifying true absences. In other words the model overpredicts presences somewhat, I think. This can be explained by other factors causing absences. Worth a comment?

We thank the reviewer for this insightful comment! We added this observation to the result and discussed it briefly after.

L398-400 : In addition, the sensitivity of the models was on average higher than their specificity (mean sensitivity and inter-quartile: 0.83 [0.79,0.90], specificity: 0.47 [0.39,0.58]), indicating a pattern of over-predicting presence over absence.

L521-523 : We noted an average higher sensitivity of the model than specificity, highlighting the over-predicting trend of our models. This might be caused by constraints that safety margins could not catch, such as higher competition in species hot margins (Sexton et al., 2009).

L432 needs rewriting and needs to be more explicit. Which Results? Fig 2? The order of regression is reversed.

Figure S7: Regression plot of LT50 against climatic niche extremes. actually, this is climate extremes regressed against LT50, in conventional terms. This is the flipside of Fig 2.

Supp Fig 8: is this meant to accompany Fig 2? shouldn’t the axes on the scatter plots be swapped? That is, explaining P50 with the climatic niche variables as predictors? and why fit GAM when you report linear coefficients?

The reviewer rightly noted that the figures and text in this section were not sufficiently explicit and linked to the main text. We added the reference to the main text and changed the figure

to display linear models only, and flipped the axis to accurately represent the effect size of Fig. 2.

For Review Only